NASA CONTRACTOR
REPORT

NASA CR-129035

RADIOISOTOPE TRACER STUDIES IN THE NASA SKYLAB EXOTHERMIC BRAZING EXPERIMENT M-552

By D. N. Braski, H. L. Adair, and E. H. Kobisk

Oak Ridge National Laboratory
Oak Ridge, Tennessee 37830

September 1974

Prepared for

NASA-GEORGE C. MARSHALL SPACE FLIGHT CENTER
Marshall Space Flight Center, Alabama 35812

TECHNICAL REPORT STANDARD TITLE PAGE

1. REPORT NO.	2. GOVERNMENT ACCESSION NO.	3. RECIPIENT'S CATALOG NO.
NASA CR-129035		

4. TITLE AND SUBTITLE	5. REPORT DATE
Radioisotope Tracer Studies In the NASA Skylab Exothermic Brazing Experiment M-552	September 1974
	6. PERFORMING ORGANIZATION CODE
7. AUTHOR(S)	8. PERFORMING ORGANIZATION REPORT #
D. N. Braski, H. L. Adair, E. H. Kobisk	
9. PERFORMING ORGANIZATION NAME AND ADDRESS	10. WORK UNIT NO.
Oak Ridge National Laboratory Oak Ridge, Tennessee 37830	11. CONTRACT OR GRANT NO. W-74-5-eng-26
12. SPONSORING AGENCY NAME AND ADDRESS	13. TYPE OF REPORT & PERIOD COVERED
National Aeronautics and Space Administration Washington, D. C. 20546	Contractor Report
	14. SPONSORING AGENCY CODE

15. SUPPLEMENTARY NOTES

16. ABSTRACT

The first use of a radioisotope tracer for mapping flow patterns during brazing of metal components in a space environment (near-zero gravity) proved successful. A nickel ferrule was brazed to a nickel tube with Lithobraze BT (71.8% Ag, 28% Cu, 0.2% Li) which contained a trace amount of radioactive ^{110}Ag. Mapping of the flow of the braze alloy in the annulus formed between the tube and the concentric ferrule was determined by counting the radiation intensity as a function of position in the braze joint. Significant information concerning the thermal history of the braze was determined which would have otherwise been unknown without radioisotope mapping.

17. KEY WORDS	18. DISTRIBUTION STATEMENT
	Unclassified - Unlimited

19. SECURITY CLASSIF. (of this report)	20. SECURITY CLASSIF. (of this page)	21. NO. OF PAGES	22 PRICE
Unclassified	Unclassified	51	NTIS

ACKNOWLEDGMENTS

The authors appreciate the excellent support of Bill Leslie and his coworkers in performing autoradiography, metallography, and initial sectioning work, and C. R. Richard along with Claude Benge, for final EDM sectioning of the actual Skylab flight samples. Special thanks are also due Anne Farris for preparation of the final report.

TABLE OF CONTENTS

	Page
SUMMARY	1
INTRODUCTION	2
PROCEDURE	2
Irradiation of Braze Alloy Tracer Pellets	2
$^{110m-110}$Ag Decay Scheme	5
Loading ^{110}Ag Tracer Pellets into Braze Assemblies	6
ANALYSIS AND DISCUSSION - GROUND-TEST SAMPLES	8
X-Ray Radiographs	8
Autoradiographs	8
Sectioning	11
Autoradiographs of Ring Sections	13
Isotope Tracer Maps	13
Discussion	22
ANALYSIS AND DISCUSSION - SKYLAB-II FLIGHT SAMPLES	25
Radiographs	25
Autoradiographs	27
Helium Leak Testing	27
Sectioning	29
Radiation Intensity Maps	32
Discussion	35
CONCLUSIONS	36
APPENDICES	37
REFERENCES	44

LIST OF ILLUSTRATIONS

Figure	Title	Page
1	NASA M-552 Braze Assembly	4
2	^{110m}Ag-^{110}Ag Decay Scheme	5
3	Braze Assembly Loading Sequence and Flight Package Assembly	7
4	Radiographs of Ground-Tested Braze Assemblies	9
5	Autoradiograph of IMN-2	10
6	Photomacrograph and Autoradiograph of Ring Section IMN-1, 2	12
7	Radiation Counting Apparatus	14
8	Schematic of Counting Chamber	15
9	Radiation Intensity Map for MCN-1	17
10	Radiation Intensity Map for IMN-1	18
11	Radiation Intensity Map for MCN-3	20
12	Radiation Intensity Map for IMN-2	21
13	Radiation Intensity Map for MCN-4	23
14	Radiographs of Skylab-II Assemblies SLN-2 and SLN-4	26
15	Autoradiographs of Skylab-II Assemblies SLN-2 and SLN-4	28
16	Photograph of Skylab-II Assemblies SLN-2 and SLN-4 Before Sectioning	29
17	Sectioning Plan for SLN-2	30

LIST OF ILLUSTRATIONS (Continued)

Figure	Title	Page
18	Sectioning Plan for SLN-4	31
19	Radiation Intensity Map for SLN-2.	33
20	Radiation Intensity Map for SLN-4.	34

DEFINITION OF SYMBOLS

Symbol	Definition
^{110}Ag	Silver isotope, atomic weight = 110
^{110m}Ag	Metastable silver isotope, atomic weight = 110
μCi	Microcuries
MeV	Mega (million) electron volts
ORNL	Oak Ridge National Laboratory

RADIOISOTOPE TRACER STUDIES IN THE NASA SKYLAB EXOTHERMIC BRAZING EXPERIMENT M-552*

SUMMARY

With the intent of mapping the movement of braze alloy in the joining of a nickel tube and ferrule, a radioisotope (^{110m}Ag) was used as a tracer. The experiment, NASA Skylab M-552, was designed to observe differences in the brazing of metals in a space environment (near-zero gravity) as compared with a similar braze on earth. The braze alloy used in this experiment, Lithobraze BT, has a composition of 71.8% Ag, 28% Cu, and 0.2% Li; small specimens of the braze alloy were irradiated with thermal neutrons in an ORNL reactor to obtain trace quantities of ^{110m}Ag isotope. Specific location of a small irradiated specimen in one ring of nonirradiated braze alloy, used to braze the tube and ferrule assembly, permitted tracing of ^{110m}Ag concentration gradients in the finished braze through sectioning and direct radiation counting of the braze joint. Concentration gradients were then related to the braze flow patterns under molten conditions.

Flow of the braze alloy in the annulus formed by the tube and ferrule appeared dependent on forces of gravity, capillary action, and the thermal history of the melting process when the experiment was performed on earth. In contrast, capillary action and thermal history seemed to be the dominating force factors operating in the space environment of Skylab. In both unit and near-zero gravity experiments, flow of braze material into "hot zones", generated by uneven ignition of the thermite-type heat powder during the initial stages of the braze, was evident. This phenomenon would not have been observed without the use of the radioisotope tracer-containing alloy.

---

*Research sponsored by the U. S. Atomic Energy Commission under contract with the Union Carbide Corporation.

INTRODUCTION

This report presents the results of radioactive tracer studies conducted at ORNL for the NASA Skylab Experiment M-552. Trace quantities of the metastable silver-110 isotope (^{110m}Ag) were used to determine the distribution and flow patterns of braze material in an annulus formed between a nickel tube and a nickel ferrule. The pure nickel ferrule was formed with two grooves in which Lithobraze BT (71.8% Ag-28% Cu - 0.2% Li) alloy was positioned. The annular clearance between the tube and the ferrule before brazing was, for the isotope tracer studies, either a uniform 0.010 in. (0.025 cm) or a longitudinal taper clearance from 0.000 to 0.030 in. (0.000-0.076 cm). Pellets of Lithobraze BT were neutron-irradiated at ORNL so that trace quantities of ^{110m}Ag atoms were formed and one such pellet was inserted in one of the braze alloy grooves together with inactive braze material. The braze assemblies were subsequently heated above the melting point of the braze alloy by firing an exothermic reactive mixture surrounding the assembly; brazing was performed at the Marshall Space Flight Center (MSFC), Huntsville, Alabama, and in Skylab II (1973). Upon melting, the braze alloy flowed into the annulus between the tube and the ferrule and, after cooling, the assemblies were machine cut into transverse sections for analysis. Radioisotope tracing consisted of measuring the intensity of radiation from the silver isotope at numerous points around the braze filled annulus in each transverse section. Individual radiation intensity results (for all sections) were then combined to generate a two-dimensional radiation intensity map of the entire braze joint. Finally, the intensity maps for assemblies brazed on earth were compared with those brazed on Skylab II in a near-zero gravity environment.

PROCEDURE

Irradiation of Braze Alloy Tracer Pellets

The Lithobraze BT used in Skylab M-552 experiments had a composition of 71.8% Ag, 28% Cu, and 0.2% Li, a melting point of 754°C, and a flow point of 760°C. Small rectangular pellets of this material, approximately 4.7 mm x 4.0 mm x 1 mm thick, were irradiated in the Bulk Shielding Reactor (BSR) at ORNL. On October 17, 1972, the first group of pellets (AG-1) were subjected to a flux of 1.5×10^{12} thermal neutrons/cm^2 · sec for 20 hours, while a second group (AG-2) was irradiated for 10 hours in a flux of 5.5×10^{12} thermal neutrons/cm^2 · sec. Neutron irradiation produced $^{110m-110}$Ag as well as isotopes of copper in

the braze pellets. Following irradiation, all tracer pellets were stored for several days to allow the shorter half-life copper isotopes to decay to insignificant activity levels. The radiation intensity from each pellet was measured on October 31, 1972, in a 4-π geometry high pressure ionization chamber (ORNL); results of these measurements showed that pellets in the AG-1 and AG-2 groups contained approximately 28 μCi and 50 μCi, respectively, of the ^{110m}Ag isotope. Table 1 lists each tracer pellet, its contained concentration of ^{110m}Ag, the dates when the concentrations were measured, the NASA braze assemblies into which the pellets were loaded, and finally, the dates when the assemblies were loaded. A schematic drawing of the entire braze assembly is shown in Fig. 1.

Table 1. ^{110}Ag Tracer Pellet Data

Pellet No.	Activity (μCi)	Date Measured	NASA Braze Assembly No.	Date Loaded
1AG-1	26.0	10-31-72	MCN-1	10-31-72
2AG-1	28.0	10-31-72	MCN-4	10-31-72
3AG-1	29.0	10-31-72	-	-
1AG-2	47.1	10-31-72	MCN-2	10-31-72
2AG-2	47.3	10-31-72	MCN-5	10-31-72
3AG-2	55.3	10-31-72	SLN-2	12-19-72
4AG-2	51.3	10-31-72	IMN-1	10-31-72
5AG-2	51.6	10-31-72	IMN-2	10-31-72
6AG-2	48.9	10-31-72	MCN-3	10-31-72
7AG-2	48.2	10-31-72	MCN-6	10-31-72
12AG-1	27.0	11-29-72	Film Check	11-19-72
14AG-1	25.5	11-19-72	Film Check	11-29-72
11AG-2	48.6	12-18-72	SBN-2	12-19-72
12AG-2	47.3	12-18-72	SBN-4	12-19-72
13AG-2	45.7	12-18-72	SLN-4	12-19-72

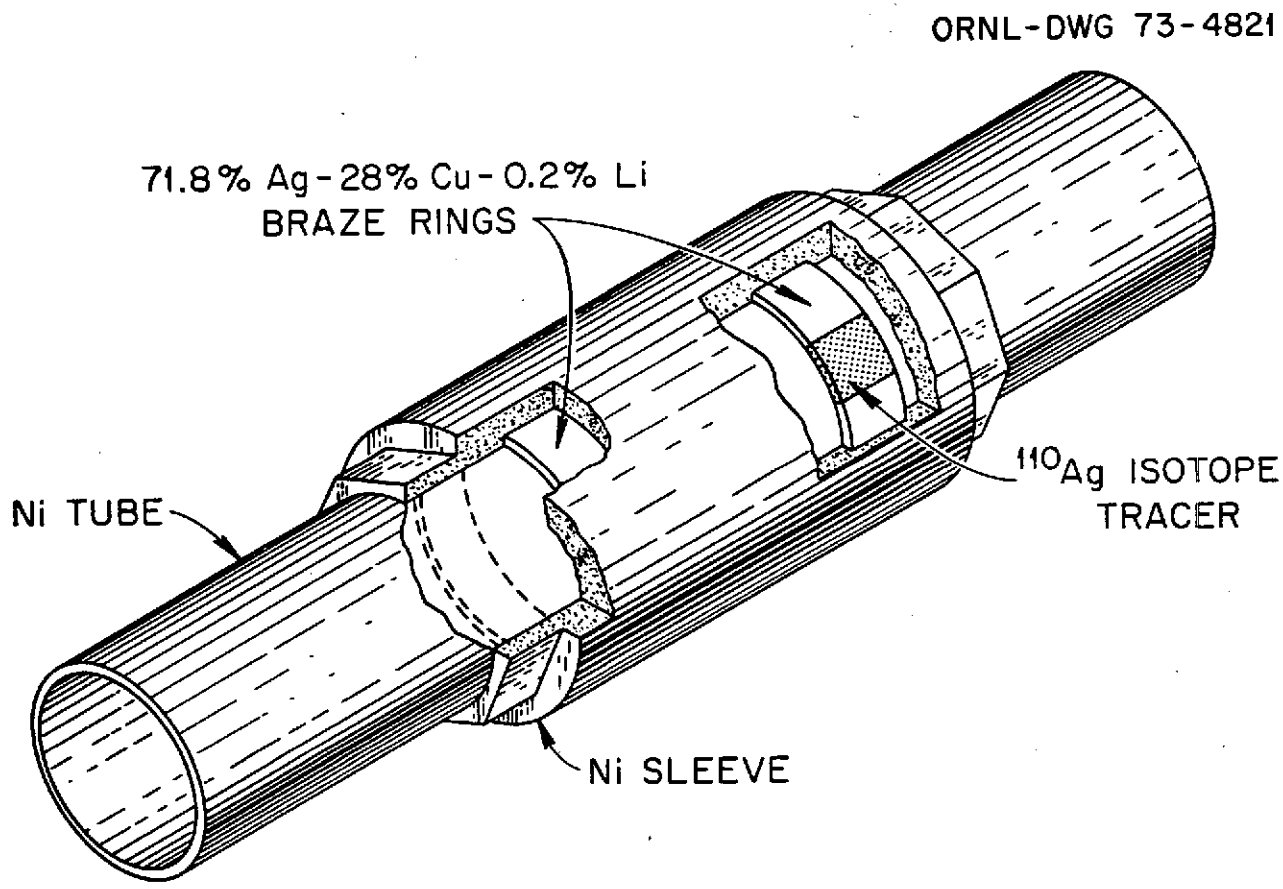

Figure 1. NASA M-552 Braze Assembly

^{110m}-^{110}Ag Decay Scheme

A simplified schematic drawing depicting the main features of the ^{110m}Ag decay scheme[1] is shown in Fig. 2. The ^{110m}Ag isotope has a half-life of 253 days. Ninety-five percent of the isotope decays by emission of a 0.087 and a 0.53 MeV β-particle together with a series of gamma radiations of various energies until the ^{110}Cd ground state is reached. (Many of the gamma-emitting transitions are not shown in the figure, but may be found in Ref. 2 or other such handbooks.) Five percent of the ^{110m}Ag decays by isomeric transition to ^{110}Ag which has a half-life of only 24 sec. The ^{110}Ag decays directly to ^{110}Cd by emitting β-particles having energies of 2.87 MeV and 2.18 MeV and a γ-ray of 0.656 MeV. For simplicity, the ^{110m}Ag-^{110}Ag isotopes and their associated decay scheme will be referred to as ^{110}Ag throughout the remainder of this report.

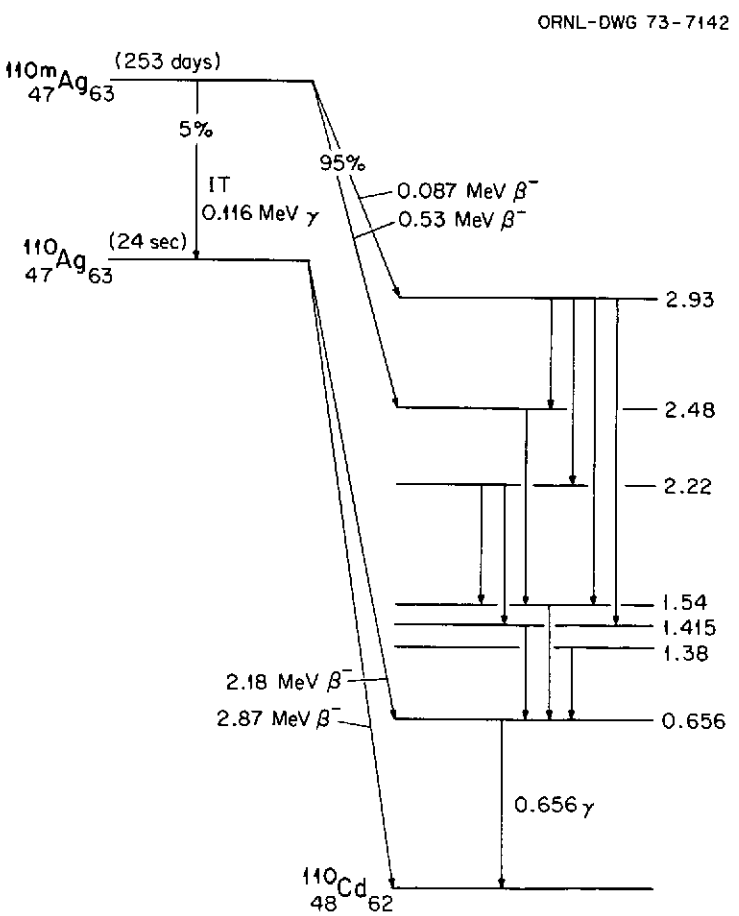

Figure 2. ^{110m}Ag-^{110}Ag Decay Scheme

Loading ^{110}Ag Tracer Pellets into Braze Assemblies

The loading of ^{110}Ag tracer pellets into the assemblies took place at ORNL, but all of the hardware and some of the personnel involved were supplied by NASA. The procedure used to load the ^{110}Ag tracer pellets into the braze assemblies is illustrated in Fig. 3. In the first step, a pair of modified snap-ring pliers were used to spread the split braze ring located in the nickel ferrule, thus creating a small slot into which a tracer pellet was inserted using tweezers (Fig. 3a). The nickel tube was then inserted into the ferrule such that the pellet was located beneath the double longitudinal scribed lines on the ferrule and at the end nearest the double radially scribed lines on the nickel tube. These scribed lines enabled immediate location of the original tracer pellet position when constructing isotope tracer maps of the finished braze. Four of the braze assemblies were placed in a flight package as shown in Fig. 3b. Of the four assemblies, only two contained ^{110}Ag tracer pellets and were located as shown in the flight package. The remaining two assemblies were fabricated from 304 L stainless steel components rather than nickel and were to be used for metallurgical studies conducted by other investigators. Figure 3c shows the igniter wire board being soldered to the package, while Fig. 3d shows the outer lid being attached. This completed the loading procedure conducted at ORNL and the flight package was ready for installation in Skylab II. Table 1 lists the braze assemblies and the dates they were loaded with ^{110}Ag tracer pellets. Those assembled in October 1972 were used for ground-based or unit gravity tests while those loaded in December 1972 were designated for the Skylab or near-zero gravity experiments. Assemblies designated SLN-2 and SLN-4 were the Skylab flight samples, while samples SBN-2 and SBN-4 were backup assemblies.

To check the possible effect of ^{110}Ag radiation on photographic film in Skylab-II, two braze assemblies were loaded with 12AG-1 and 14AG-1 pellets (see Table 1) and placed in a flight package. Cans of photographic film were then placed at various distances from the flight package and exposed for 48 hours. Results of this test, as reported by NASA, illustrated conclusively that the effect of the 48-hr radiation exposure was of negligible concern and that the presence of radioactivity at this level would not cause deleterious effects to components aboard Skylab.

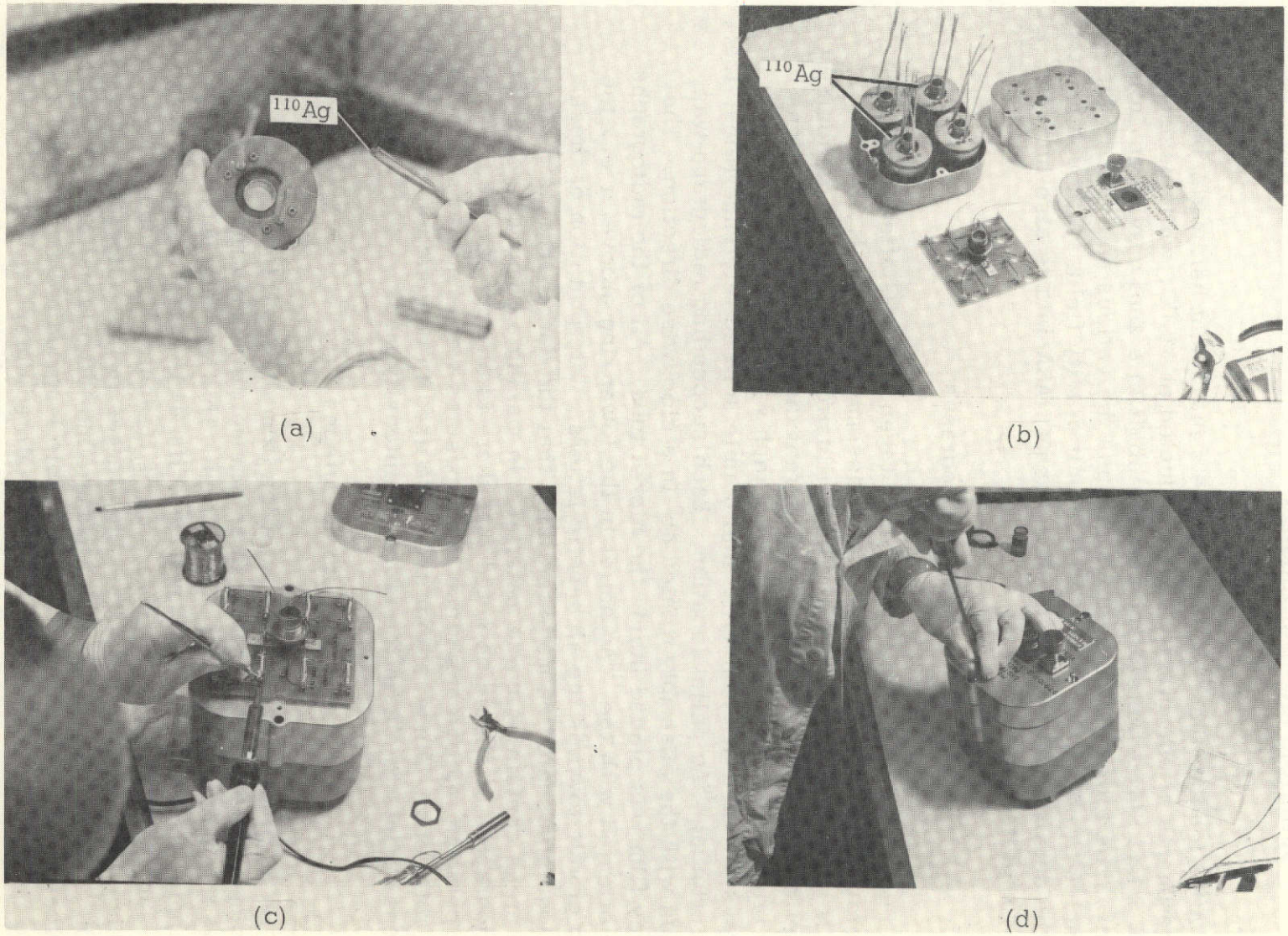

Figure 3. Braze Assembly Loading Sequence and Flight Package Assembly

ANALYSIS AND DISCUSSION - GROUND-TEST SAMPLES

After loading the ^{110}Ag tracer pellets into flight hardware, brazing experiments at unit gravity were conducted at MSFC, while assemblies SLN-2 and SLN-4 were brazed on Skylab-II in a zero gravity environment. The following paragraphs discuss the various analyses of the samples after they were brazed in a unit gravity field. Although most of the data was generated at ORNL, some NASA data is also included for completeness.

X-Ray Radiographs

Figure 4 shows x-ray radiographs taken at MSFC after completion of ground-based brazing tests using assemblies MCN-1, IMN-1, MCN-3, IMN-2, and MCN-4. Each illustrated radiograph is actually a series of radiographs taken at different circumferential locations on the braze assembly. The "0°" radiograph was taken with incident x-rays directed at the longitudinal double scribed reference lines, i.e., the original ^{110}Ag pellet location. Each succeeding radiograph was taken with the assembly rotated 45° in a clockwise direction. The x-ray film was placed inside the nickel tube. All of the radiographs are oriented with the ^{110}Ag pellet in the lower ring groove, i.e., the ring groove towards the alphabetic letters. Interpretation of these radiographs should be made realizing that the darker regions represent the areas containing braze material. In making a composite of these radiographs, it should be noted that there is an approximate 58% overlap between radiographs since the exposures were made at successive 45° rotations. These radiographs were used in conjunction with isotope intensity data to obtain the radiation intensity maps.

Autoradiographs

An autoradiograph (using radiation from the contained ^{110}Ag isotope) was made of assembly IMN-2 in an attempt to nondestructively determine the approximate ^{110}Ag distribution. This was accomplished by wrapping a sheet of Kodak Royal Pan Film 4141 (Estar thick base) around the sample for a total exposure time of 16 hours. The resultant autoradiograph is shown in Fig. 5. Light areas in the radiograph represent high ^{110}Ag content and are seen to surround the original pellet location indicated on the radiograph. The double longitudinal scribe marks have also been added for reference. This autoradiograph will be used when the isotope tracer map for IMN-2 is discussed.

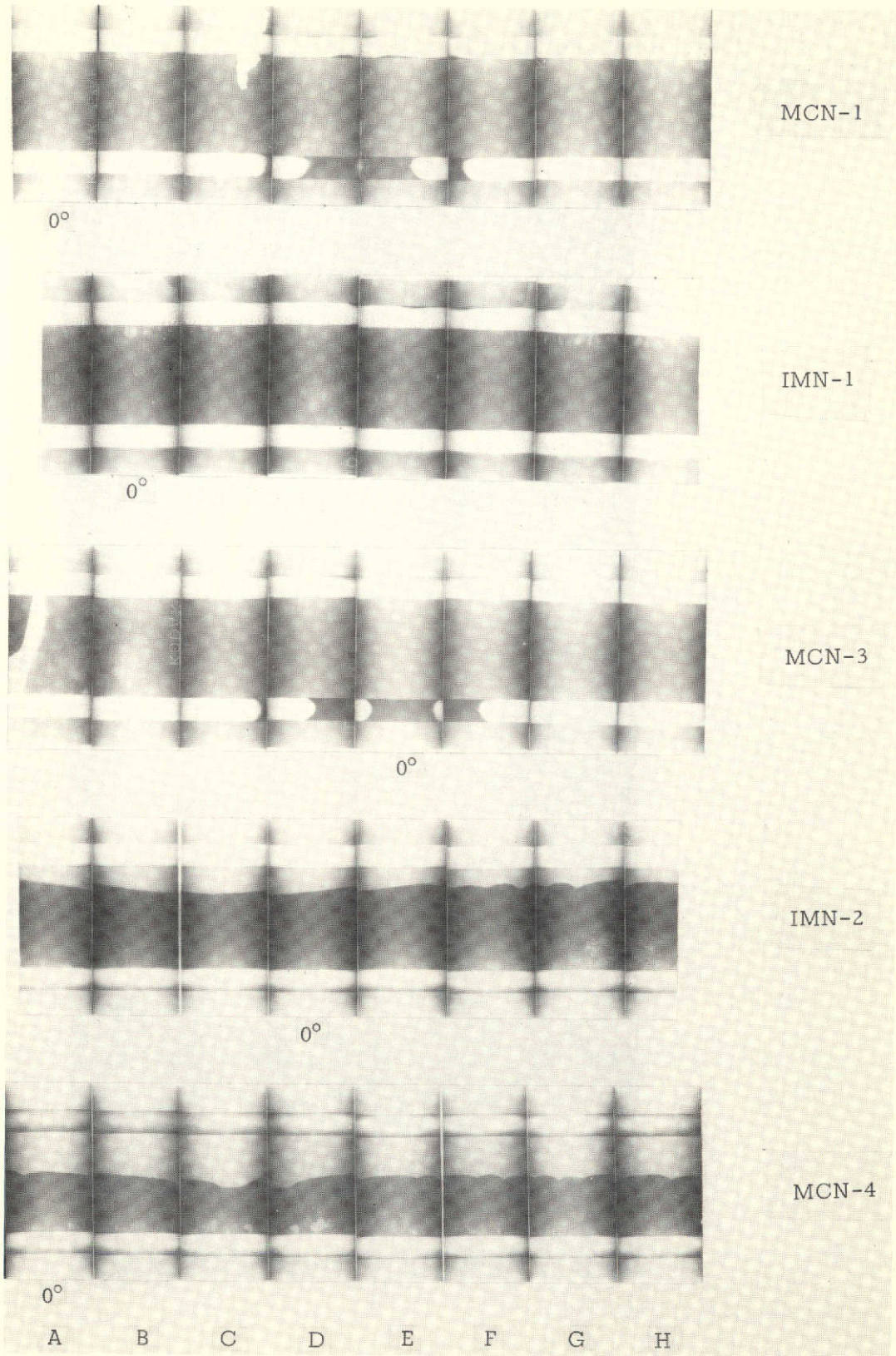

Figure 4. Radiographs of Ground-Tested Braze Assemblies

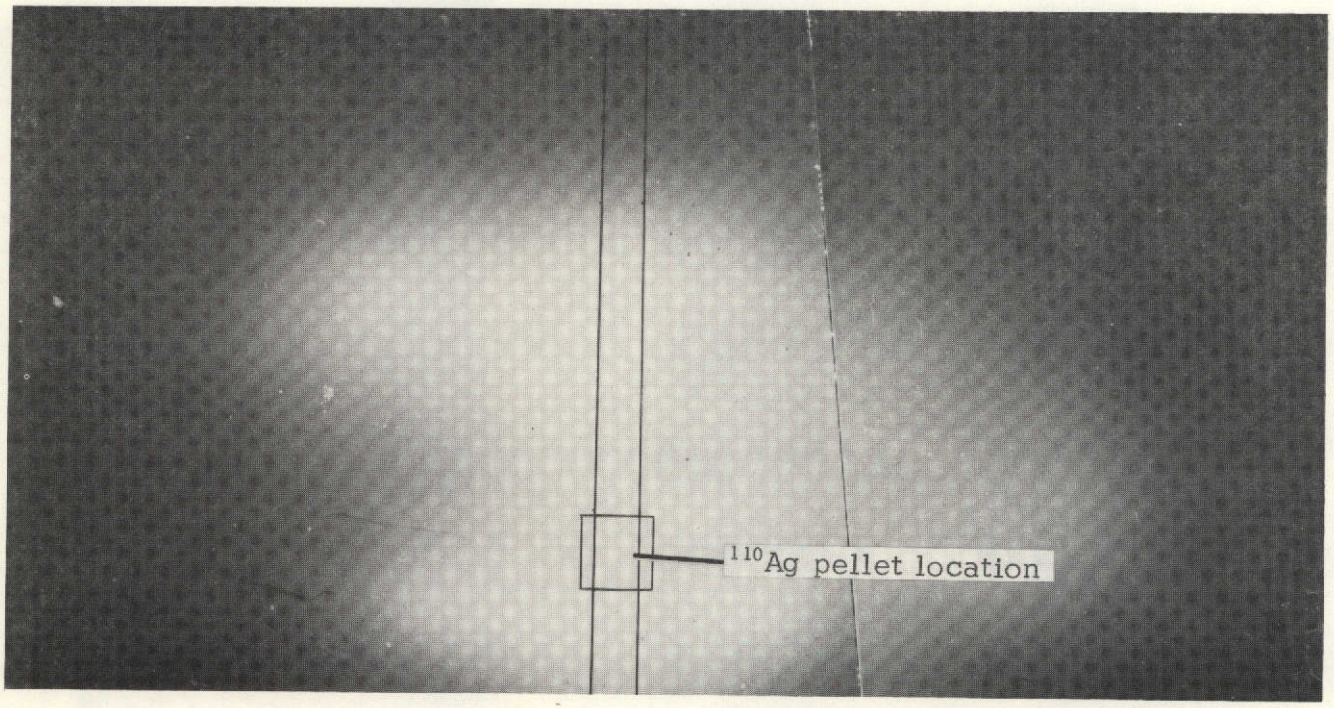

Figure 5. Autoradiograph of IMN-2

Sectioning

Table 2 lists the methods by which braze assemblies were sectioned into rings, to facilitate radiation mapping, and also the laboratories where sectioning was performed. An abrasive cut-off wheel was used to section samples MCN-1, MCN-4, and MCN-3, at Battelle Memorial Institute (BMI). Initial sectioning at ORNL on IMN-1 was performed with a 1-mm thick silicon carbide cut-off wheel and water coolant. Because of difficulties in making parallel cuts in the relatively soft nickel tubing using the cut-off wheel technique, sample IMN-2 was sectioned using a lathe and a 0.75-mm wide hardened steel cut-off tool. Sectioning of MCN-1 and MCN-4 was also conducted using a lathe. Sectioning the soft nickel by the lathe technique presented a problem in that the cut surfaces contained some cold-worked metal. These surfaces were later etched in aqua regia for 2 min. to remove the cold-worked areas before radiation counting was carried out. Finally, Skylab samples SLN-2 and SLN-4 were sectioned by electrical discharge machining (EDM) which will be described in the analysis section concerning these samples.

Table 2. Sectioning Methods

NASA Braze Assembly No.	Method Sectioned	Laboratory Where Sectioned	Date of Section Counting	Sectioning Data
IMN-1	Cut-off wheel	ORNL	2-27-73	Appendix A
IMN-2	Lathe	ORNL	1-30-73	Appendix B
MCN-1	Cut-off wheel (3 sections)	BMI	2-12-73	Appendix C
	Lathe (6 sections)	ORNL	3-13-73	
MCN-3	Cut-off wheel (9 sections)	BMI	5-21-73	Appendix D
MCN-4	Cut-off wheel (3 sections)	BMI	2-13-73	Appendix E
	Lathe (6 sections)	ORNL	3-7-73	
SLN-2 (Skylab-I)	Electrical discharge machining (EDM)	ORNL	7-27-73	Appendix F
SLN-4 (Skylab-I)	EDM	ORNL	7-31-73	Appendix G

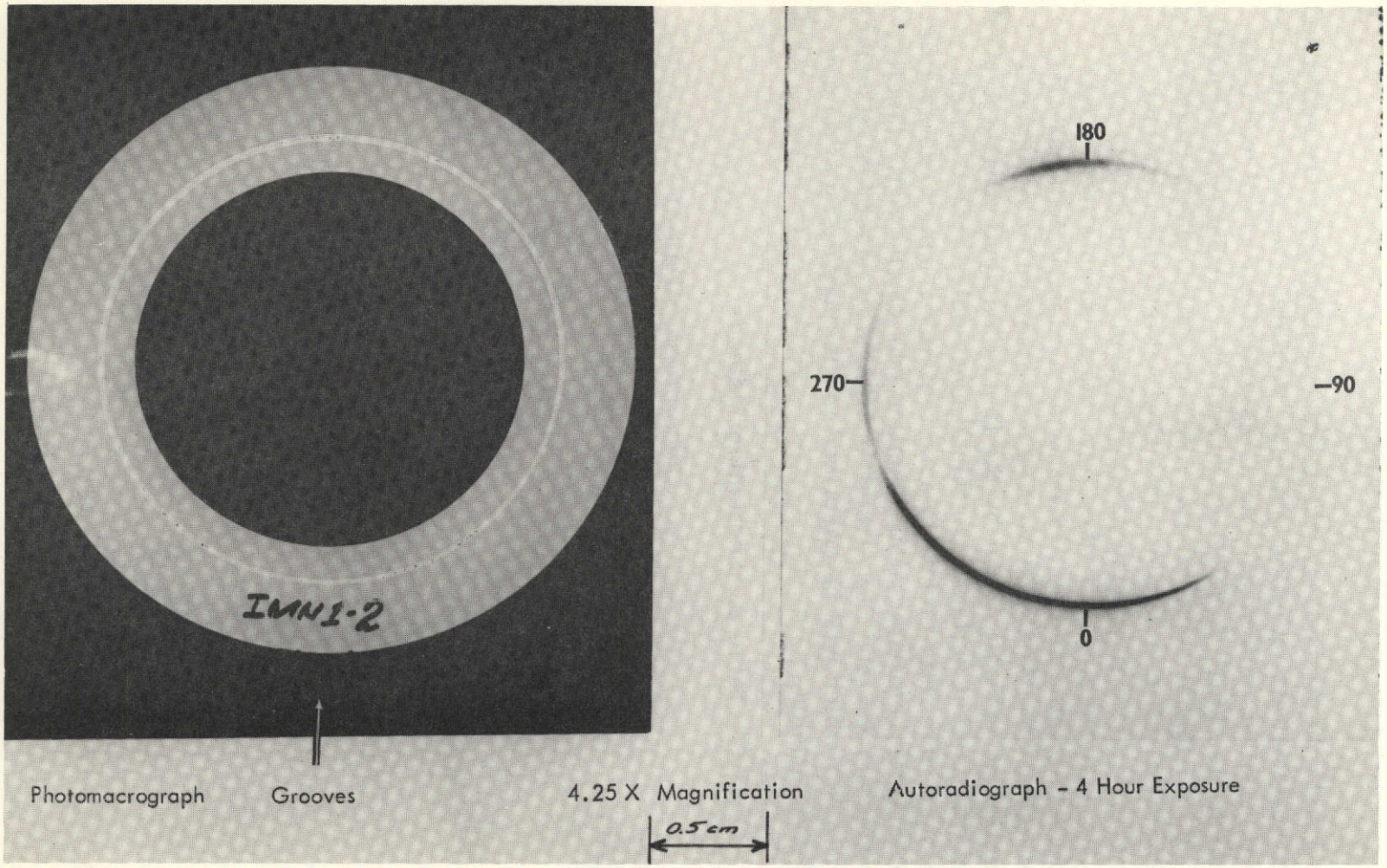

Figure 6. Photomacrograph and Autoradiograph of Ring Section IMN-1.2

Autoradiographs of Ring Sections

During the early stages of this program the sectioned rings from IMN-1 were autoradiographed and examined by the metallography group at ORNL before they were analyzed by radiation counting techniques. Typical results from this analysis are given in Fig. 6 for ring IMN-1.2. The photomacrograph on the left of Fig. 6 shows the ring after metallographic mounting and polishing. The thin light colored annular band in the center of the ring is the braze material. A moderate amount of porosity is evident in the braze even at this low magnification. The double scribe marks (longitudinal) are seen at the bottom or six o'clock position of the ring. An autoradiograph of this same section is shown on the right of the figure; the radiograph was made by placing the ring, polished side down, on a plate of Kodak Nuclear Track film (NTB-2) for a total exposure time of 4 hours. The autoradiograph showed that the braze containing the radioactive tracer (dark areas) flowed circumferentially from the reference marks, the 0° azimuth, and that more isotope flowed toward the 270° azimuth than the 90° azimuth. Another area of high ^{110}Ag concentration is observed at the 190° azimuth; ^{110}Ag-deficient areas are seen near an azimuth of 90°. This autoradiograph will be referred to later and correlated with the radiation intensity map for IMN-1.

Isotope Tracer Maps

The movement of the tracer alloy during melting can be conveniently presented and studied by making a radiation intensity map of the sample. Mapping was accomplished by determining the radiation intensity from different portions of the ring sections and plotting the data in a two-dimensional fashion. The equipment used to measure intensities in the ring section is shown in the photograph in Fig. 7; on the left is a multichannel analyzer, a Nuclear Data ND812 mini-computer, a detector power supply, and auxiliary electronic instrumentation. The vacuum-counting chamber is located on the table behind the teletype readout; a schematic diagram of the counting chamber is given in Fig. 8. The detector used to measure the ^{110}Ag radiation was an ORTEC, 3.3-mm diameter silicon surface-barrier type with a minimum depletion depth of 100 microns. The detector was held by an x-y positioning fixture and, for this analysis, was aligned in a fixed position directly above the circumference of the braze ring. The ring section was mounted below on a turntable that permitted remote rotation of the section in 5° increments. With a detector diameter of 3.3 mm, the detector could

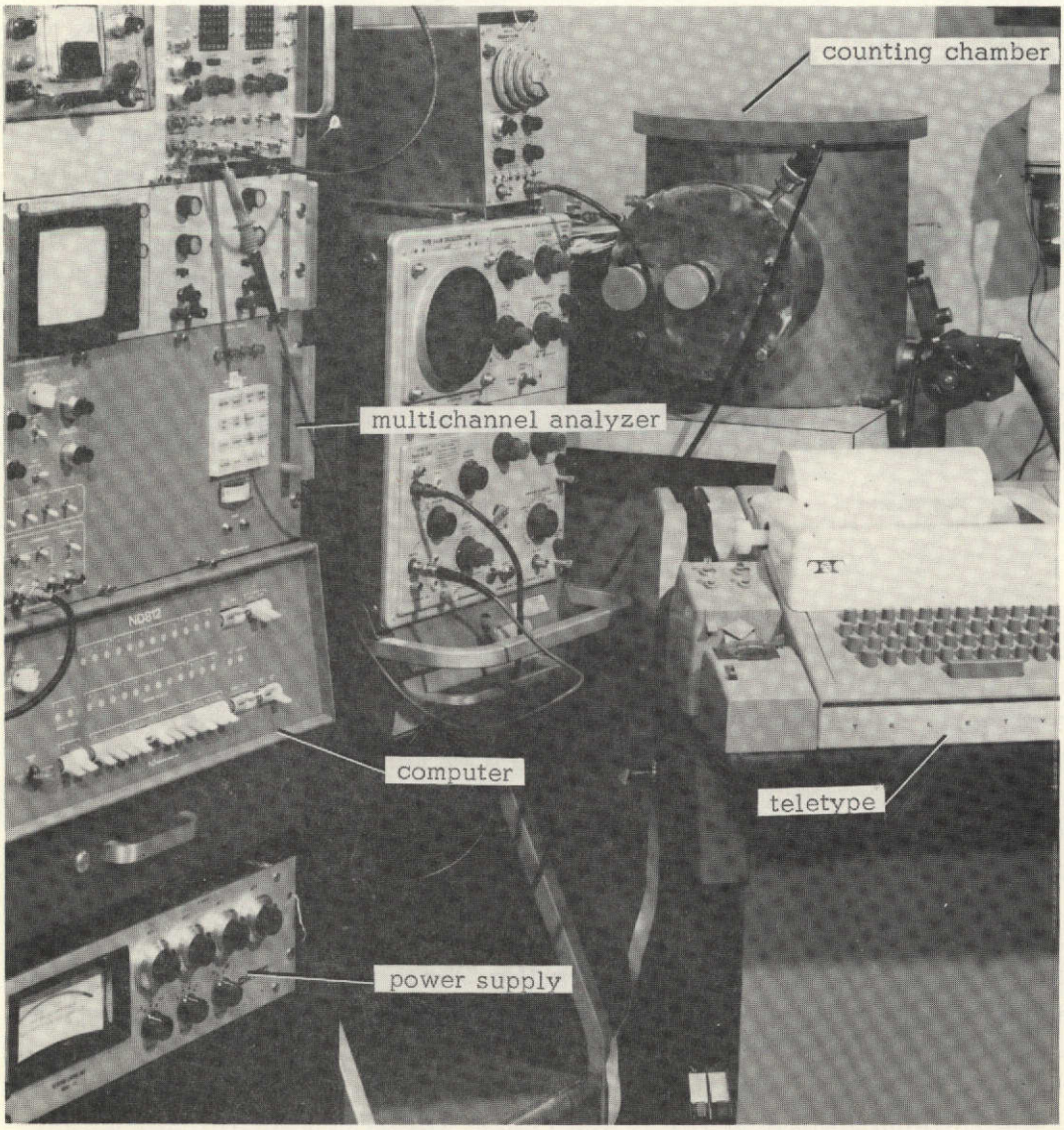

Figure 7. Radiation Counting Apparatus

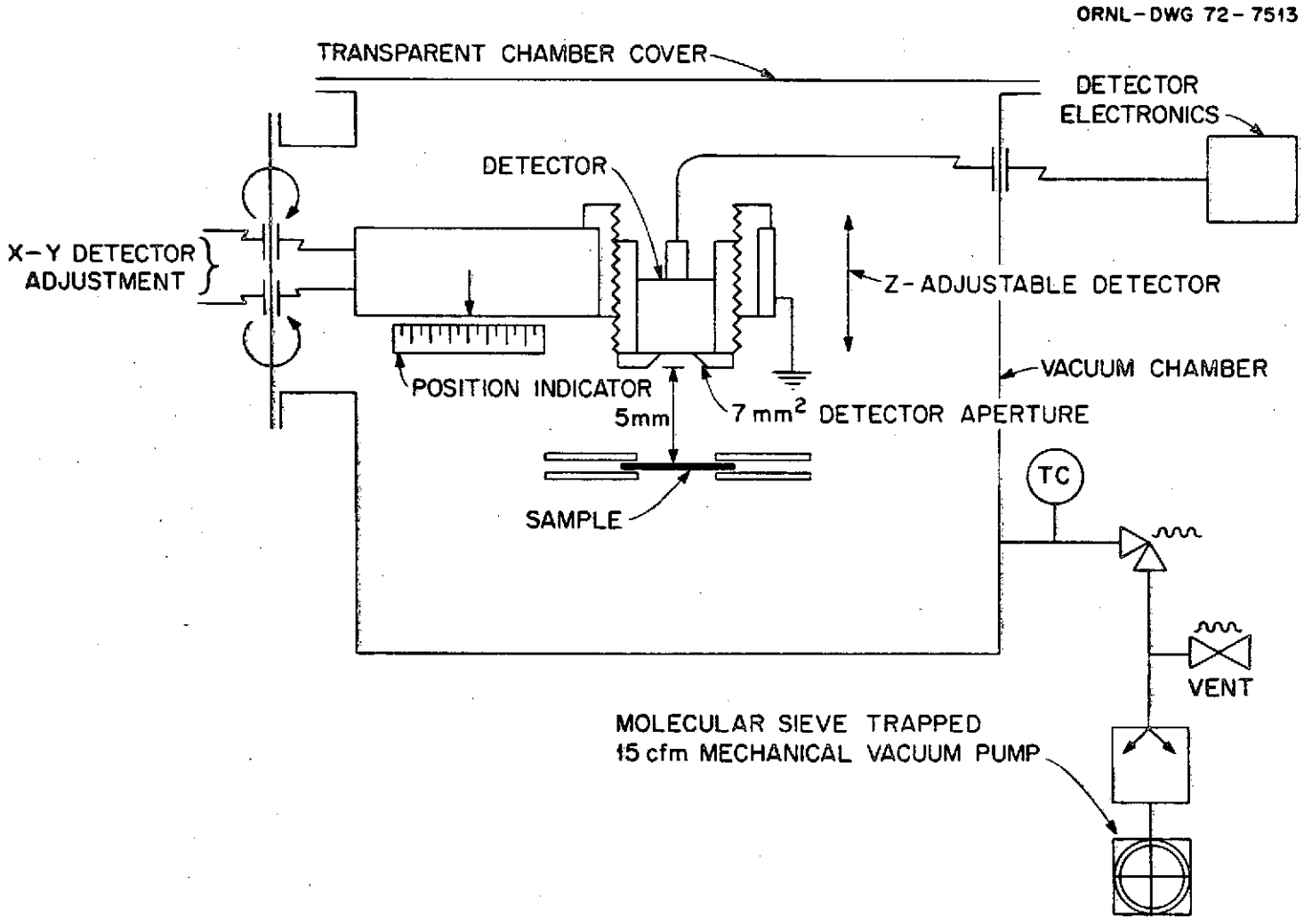

Figure 8. Schematic of Counting Chamber

survey a braze area in 20° increments of rotations with very little overlap of areas. To make the radiation intensity map, the intensity values for a 100-sec. counting time were normalized by dividing by the volume of braze being analyzed. The volume of braze material was taken as the ring section thickness (measured with a micrometer) multiplied by the gap dimension (design values) and the detector diameter of 3.3 mm. Wherever the volume of braze material was obviously different than the calculated value, an estimated correction factor was also multiplied by the volume. The volume factor for each ring section from ground-test samples is given in Appendices A through E. The final intensity concentration values have dimensions of counts/sec · in.^{3} and were plotted as a function of ring location and azimuth. (The values shown on all the intensity maps have been divided by 10^4.) Lines of iso-intensity and the original location of the ^{110}Ag pellet were then drawn to complete the map. Corresponding x-ray radiograph identification letters are also shown on each intensity map to help the reader correlate the maps with the associated radiographs in Fig. 4. The following paragraphs present and discuss the radiation intensity maps obtained from ground-test braze assemblies.

MCN-1. The intensity map for MCN-1 is shown in Fig. 9. This assembly was melted in a horizontal position with the ^{110}Ag pellet on top, in the 12 o'clock position, and had a 0.010 in. (0.025 cm) annulus clearance between the tube and the ferrule. During melting, most of the braze flowed out of both ring grooves and into the annulus; the isotope tracer flowed into the annulus on both sides of the groove, but most of it flowed towards the middle portion of the assembly. There was considerable flow of tracer material in the circumferential directions toward an azimuth of 180° or the bottom of the assembly. It should be noted that a fillet of braze material remained at the bottom of the braze alloy ring groove. No radioactivity was detected in areas that were essentially void of any braze alloy such as the upper ring groove. In regions where molten braze had wet the nickel surfaces, but were finally void of braze alloy after solidification, no residual radioactivity was observed indicating the lack of silver at the surface.

IMN-1. The IMN-1 assembly was also melted in a horizontal position, but the pellet containing the radioisotope tracer was oriented at the 3 o'clock position. In this case, the annulus width was 0.010 in. (0.025 cm). After brazing, the intensity map, Fig. 10, showed that most of the isotope tracer was found in either the central area just above the starting location or on either side of the slot from azimuthal

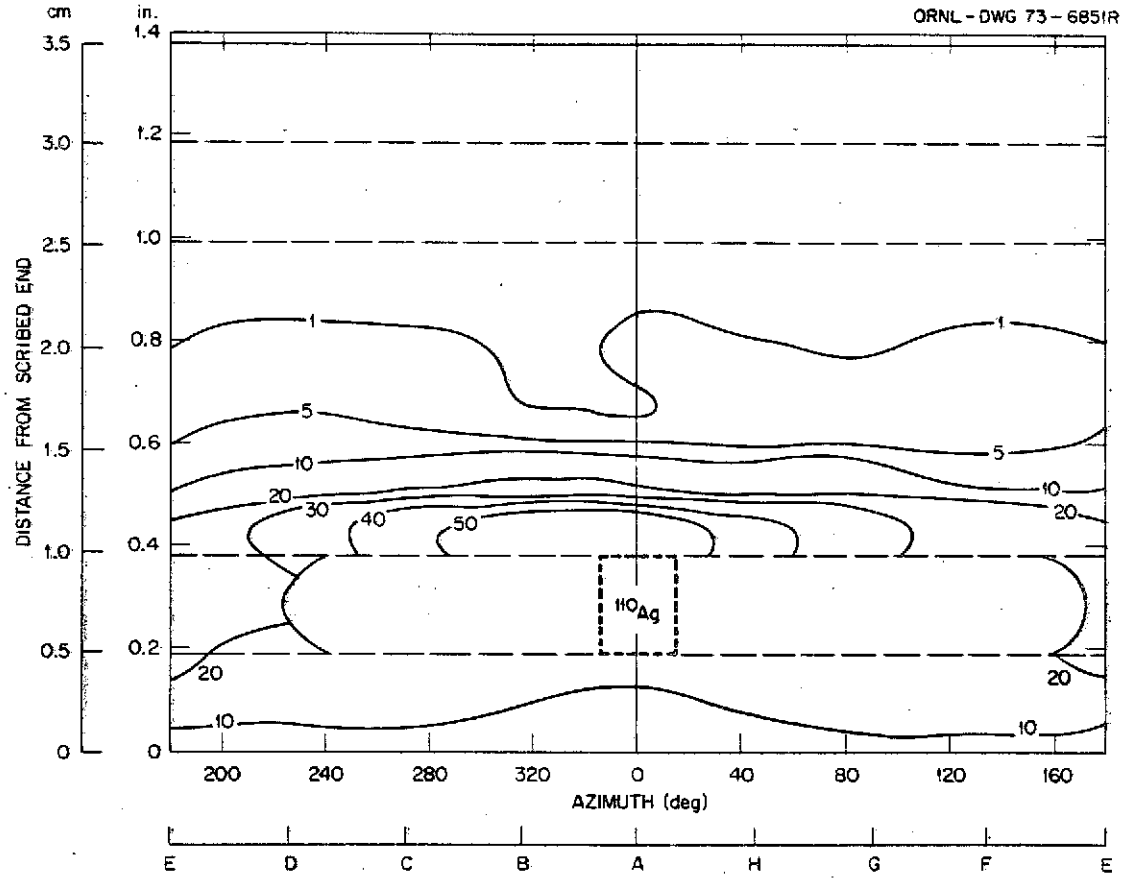

Figure 9. Radiation Intensity Map for MCN-1
Intensity units: (counts/sec · in.^{3}) x 10^{-4}

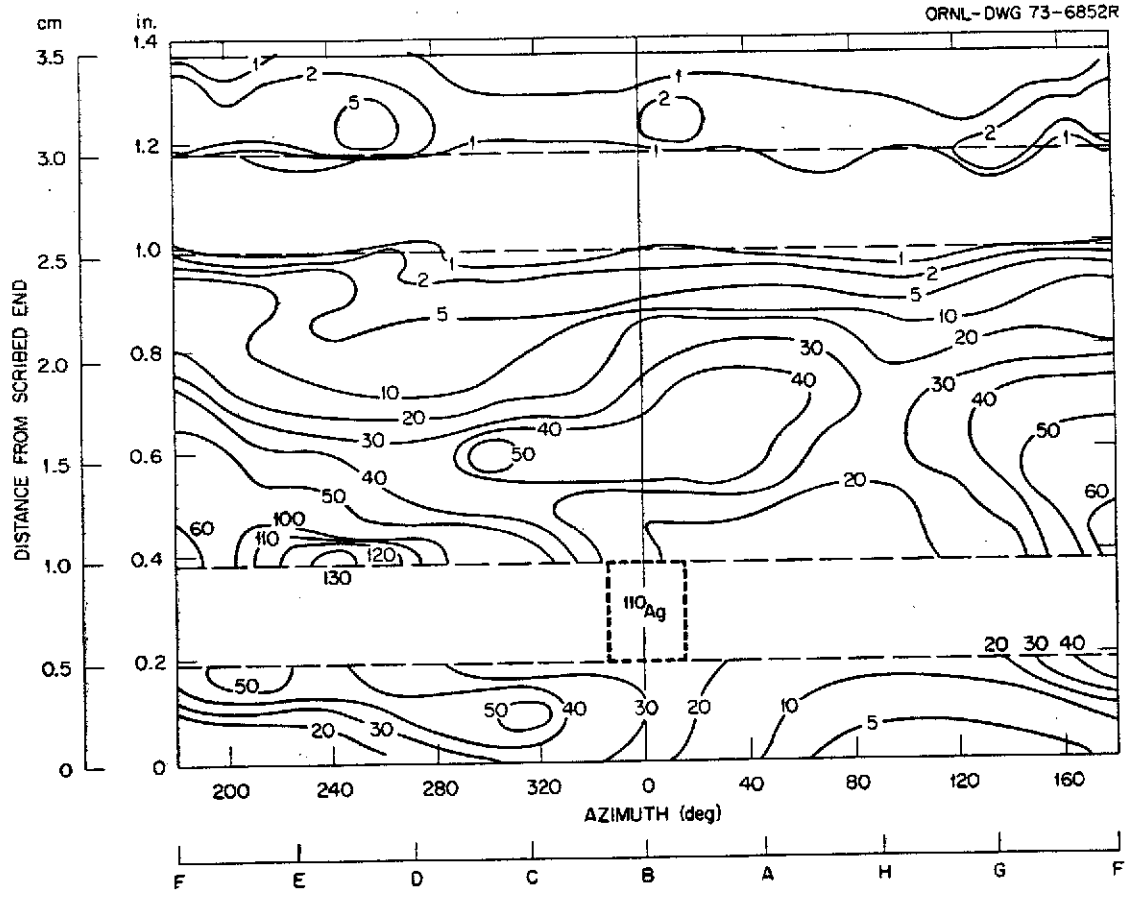

Figure 10. Radiation Intensity Map for IMN-1
Intensity units: (counts/sec · in.^{3}) x 10^{-4}

positions 0° to ~180° (moving from right to left). Flow of isotope tracer from its original position to the left on the equiintensity map corresponds to a clockwise flow of the tracer from its 3 o'clock position in the actual braze test. There are numerous "hot spots" or areas of high radiation intensity on both sides of the braze ring grooves. All of the braze alloy flowed from the grooves except for a small fillet in the upper braze groove near the 225° azimuth. A relatively high intensity reading in this area indicated that a small portion of the tracer flowed into the upper groove in that area.

There is good agreement between the radiation intensity map in the region of ring number IMN-1.2 [locator edge 0.17 in. (0.43 cm) from zero, Fig. 10] and the autoradiograph of that ring shown in Fig. 6. Both show high activity near the azimuths of 320° and 200°, while indicating low activity near the 90° azimuth. Areas between these azimuths, where radiation intensity is changing, are also consistent with the autoradiograph.

MCN-3. As with samples IMN-1 and MCN-1, the sample had an annulus width of 0.010-in. (0.025 cm) and was brazed in a horizontal position, but the tracer pellet was located in the 6 o'clock position. The isointensity map for MCN-3 (see Fig. 11) showed that much of the tracer activity remained in the area near its original location before brazing. The main flow of the tracer alloy was found to be into the annulus towards the end of the sleeve and azimuthally in both directions. Some tracer alloy flowed to an area near the second braze groove at an azimuth of 230°. All of the braze flowed out of the retaining groove regions except for a fillet near the 0° azimuth, located in the 6 o'clock position for this experiment. As before, no radioactivity was detected in areas void of braze material. Isotope tracer-deficient areas were found at an azimuth of 90° between the two retaining grooves and above the groove at the top of the map.

IMN-2. In contrast with samples described above, this braze assembly was designed with an annulus of tapered cross-section of 0.000-0.030 in. (0.000-0.076 cm) with the zero clearance below the radioisotope pellet location (double-scribed) end. The assembly was brazed vertically with the radioisotope pellet located in the bottom retaining groove. The resultant isotope intensity map, Fig. 12, shows that the tracer alloy moved into two areas: 1) immediately above the lower ring groove at an azimuth of ~310°, and 2) in the central region of the annulus near an azimuth of 20°. Care must be exercised when

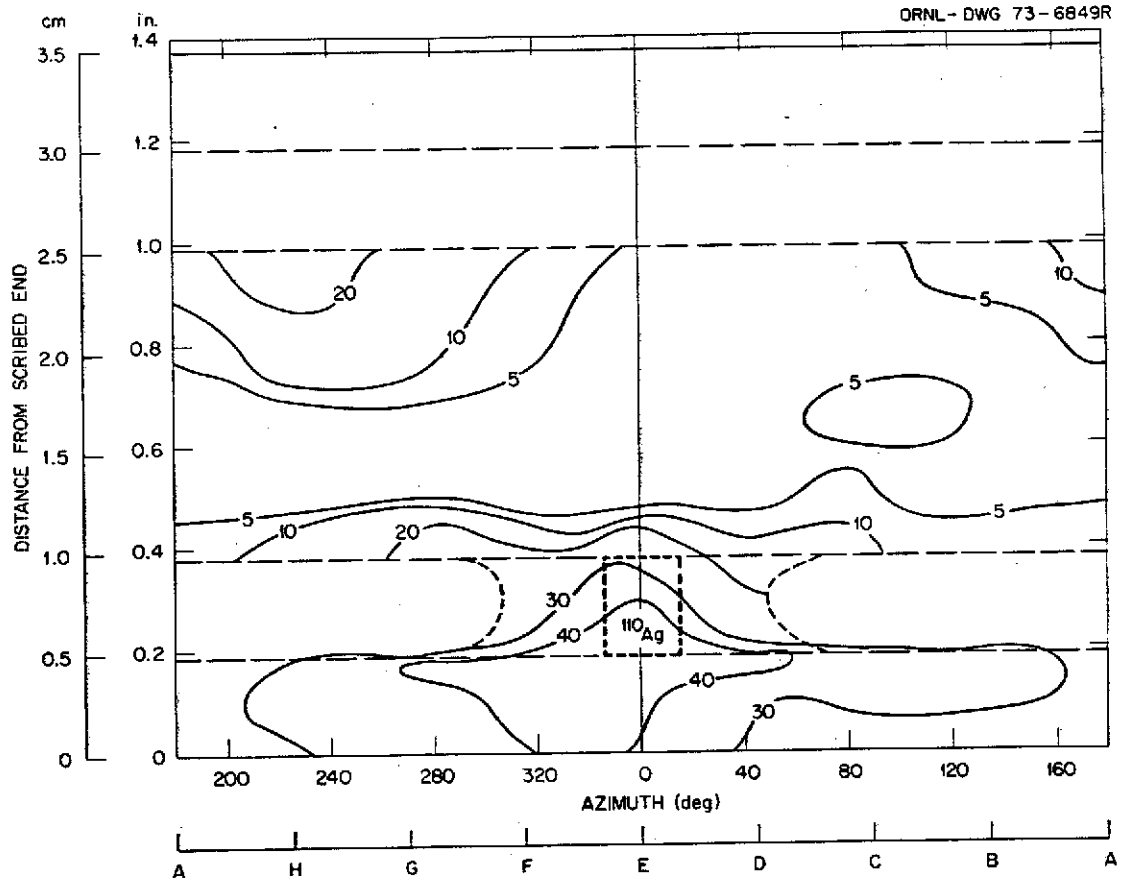

Figure 11. Radiation Intensity Map for MCN-3
Intensity units: (counts/sec · in.^{3}) x 10^{-4}

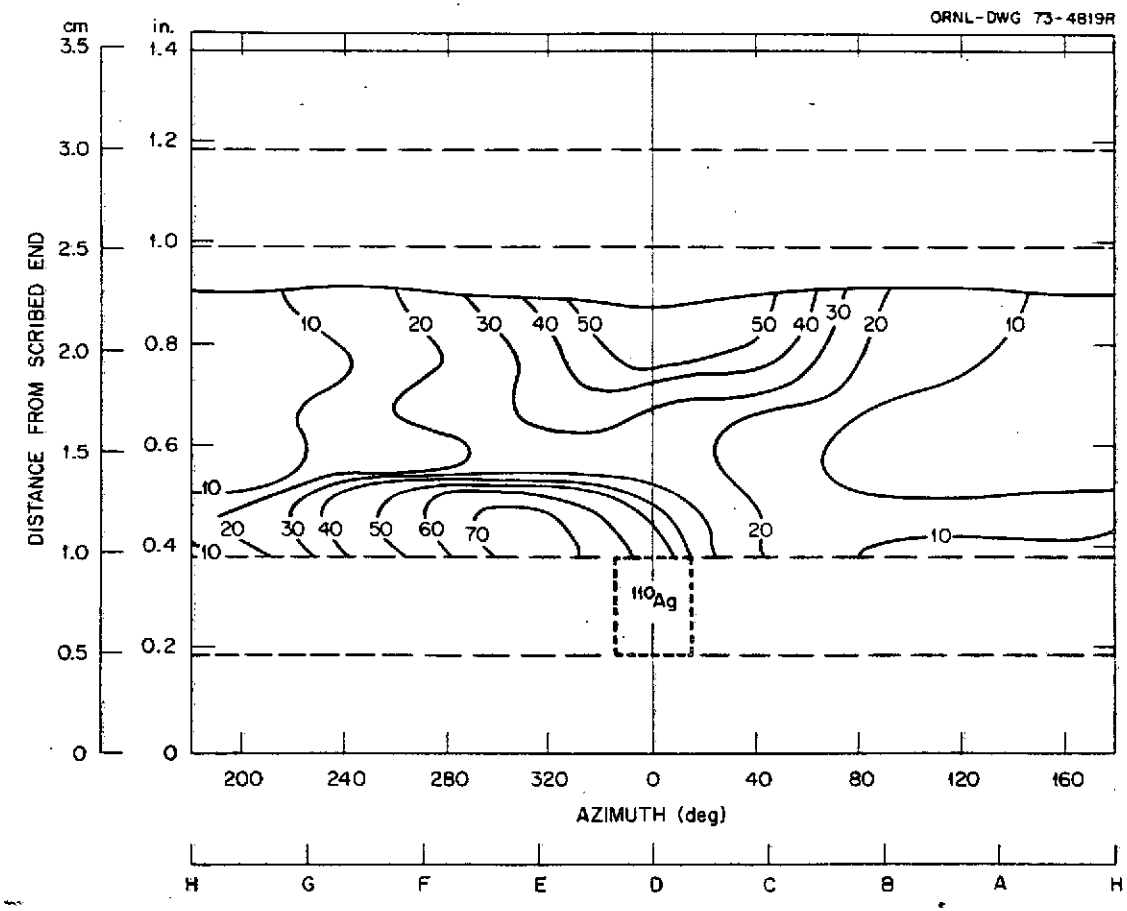

Figure 12. Radiation Intensity Map for IMN-2
Intensity units: (counts/sec · in.^{3}) x 10^{-4}

comparing intensity/unit volume values on the maps for tapered annulus samples, e.g., in Fig. 12, the isointensity line of value 70 contains substantially less total radioactivity than the line of value 50 above it as the result of annulus variation causing the incremental braze volume to be less in the "70" region than in the "50" region. In other words, the "50" region contained a larger total number of ^{110}Ag atoms than in the "70" region, but less isotope per unit volume. The ring grooves were essentially free of any braze material and only background level radiation intensity readings were measured in these areas. The annular volume below the lower braze-ring groove contained some braze material, but was not mapped because of sectioning difficulties. The braze material in these areas would be expected to contain some radioactivity, but because of the small amount of braze, the intensity would probably be relatively low. The upper level of the "braze line" is shown on the map and was taken from the radiographs shown in Fig. 4. This "water leveling" phenomena was caused by gravity acting on the vertically-brazed sample and will be seen again in sample MCN-4.

Generally, the radiation intensity map and the autoradiograph (see Fig. 5) for IMN-2 were found to be in agreement. In comparing the two radiation intensity profiles, however, the azimuth direction on the autoradiograph must be reversed since the orientation is reversed when a positive print is made of the autoradiograph negative. In other words, on the autoradiograph, one proceeds to the left of the ^{110}Ag pellet position (0° azimuth), when moving towards a 90° azimuth on the sample.

MCN-4. Sample MCN-4 was also brazed in the vertical position with the ^{110}Ag tracer pellet at the bottom. The tapered annulus (0.000-0.076 cm) was oriented with zero clearance at the bottom end. For this sample, the radiation intensity map (see Fig. 13) shows a high radiation intensity area between the braze ring grooves extending from an azimuth of approximately 220° to 0°. Most of the braze material has flowed from the braze ring grooves and these clear areas registered only background level intensities. A small amount of radioactivity was found at the bottom of the lower groove. As in the previously described sample, a braze level line due to gravity was observed and was drawn on the intensity map by referring to radiographs shown in Fig. 4.

Discussion

In a qualitative analysis of the radiation intensity maps for samples brazed in a unit gravity field, it is convenient to separate the different aspects of tracer braze flow patterns and relate them to their dominant

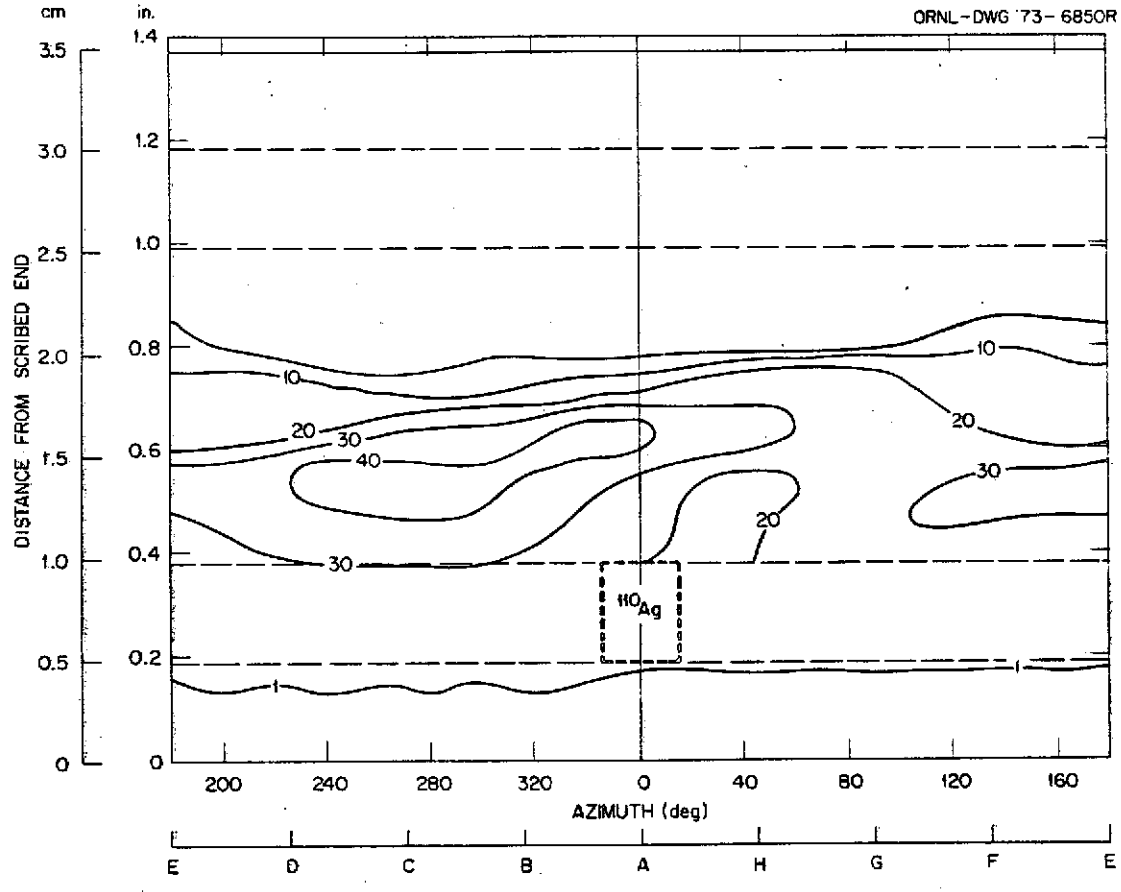

Figure 13. Radiation Intensity Map for MCN-4
Intensity units: (counts/sec · in.^{3}) x 10^{-4}

driving forces. Admittedly, this is done at the risk of oversimplification, but it is one way to make a rapid, over-all comparison of samples brazed in unit and near-zero gravity conditions. Detailed quantitative interpretation of the maps will be left to other investigators. It is felt that the salient features of the braze flow patterns can be assigned to three dominant driving forces: 1) surface forces or capillarity, 2) gravity, or 3) temperature gradients or, in general, the thermal history of the braze assembly.

Capillary action is concluded to be the main force in the movement of the molten braze alloy from the braze ring grooves into and around the annulus formed between the nickel tube and ferrule for all five assemblies (see Figs. 9-13). Capillary forces depend mainly on the gap width, surface tension of the liquid braze, viscosity of the liquid braze, wetting angle, and metal surface condition.

The effects of gravity were evident for both the horizontally and vertically brazed samples. Both samples MCN-1 and MCN-3 (Figs. 9 and 11) were brazed horizontally and were left with fillets of braze containing the radioisotope tracer at the bottom of the braze ring groove. in which the tracer pellet was originally located. In a sense, gravity and capillarity were competing forces in the earth-brazed experiments; gravity tended to "puddle" the braze alloy at the bottom of the ring groove, while capillarity tended to pull the braze into the narrow annulus. The effects of gravity can also be seen in the intensity maps for samples IMN-2 and MCN-4 (Figs. 12 and 13). The tracer alloy in these two taper-gap samples, brazed in a vertical position, was contained within a definite braze line around the interior of the annulus. This braze line or "water level" line was a direct result of gravitational force.

Thermal history associated with the braze assembly had a subtle but important effect on the flow of the isotope tracer. In all five unit gravity experiments (Figs. 9-13), there appeared to be a strong tendency for the tracer braze to flow more circumferentially, than longitudinally, inside the narrow annulus. This characteristic was especially evident for samples MCN-1, IMN-1, and MCN-4 (Figs. 9, 10, and 13, respectively). It would seem that the flow of tracer braze was influenced by thermal gradients which existed, at least initially, during the melting of the alloy. Existence of these thermal gradients might well have been caused by the manner in which the exothermic material was ignited, i.e., through the use of two igniters. For the earth-bound tests, these igniters were located at the tracer-pellet end of the assemblies, at

azimuths of 90° and 270° from the original pellet location (0°). These regions would reach the melting point of the braze alloy as well as their maximum temperatures well before other areas of the assembly reached equal thermal levels. Braze alloy would flow in these regions of highest temperature before flow could occur in the cooler regions during the initial period of the exothermic burn. It is well known, from a practical standpoint, that a braze alloy will flow into areas of higher temperature. Theoretically, the increased flow into regions of higher temperature is linked strongly to the reduction of viscosity of the liquid braze, but is also affected by other factors such as changes in the surface tension of the liquid braze, etc. In any case, it is felt that the tracer alloy tended to flow rapidly towards the 90° and 270° regions initially as the result of higher relative temperatures in these areas. Then as thermal gradients lessened, as the result of the excellent thermal conductivity of the braze alloy, subsequent movement of the tracer isotope in the liquid braze was by diffusion and convection mechanisms. However, the relatively uniform nature of the radiation intensity maps would seem to relegate these latter effects to secondary importance as compared with the initial flow patterns induced by capillarity and uneven melting of the alloy.

Results of Spearman, Muraki, and Masubuchi[3] show that a substantial temperature gradient existed in the axial direction inside the nickel tube, with highest temperatures located near the center of the assembly. Upon combining this thermal gradient with those expected from local heating associated with the igniters, one would expect that the preferential flow of the tracer alloy would be into the annulus and towards the 90° and 270° azimuth regions. Radioisotope tracer maps for the ground-tested braze assemblies (Figs. 9-13) generally follow this trend.

ANALYSIS AND DISCUSSION - SKYLAB II FLIGHT SAMPLES

Radiographs

Radiographs of Skylab samples SLN-2 and SLN-4 were taken at MSFC and are shown in Fig. 14. These radiographs were taken at 45° intervals around the inside of the assemblies with respect to the longitudinal double scribe mark in the "A" radiograph. It should be noted that, unlike the radiographs presented for the ground tests, the light areas are reversed and correspond to areas containing braze material.

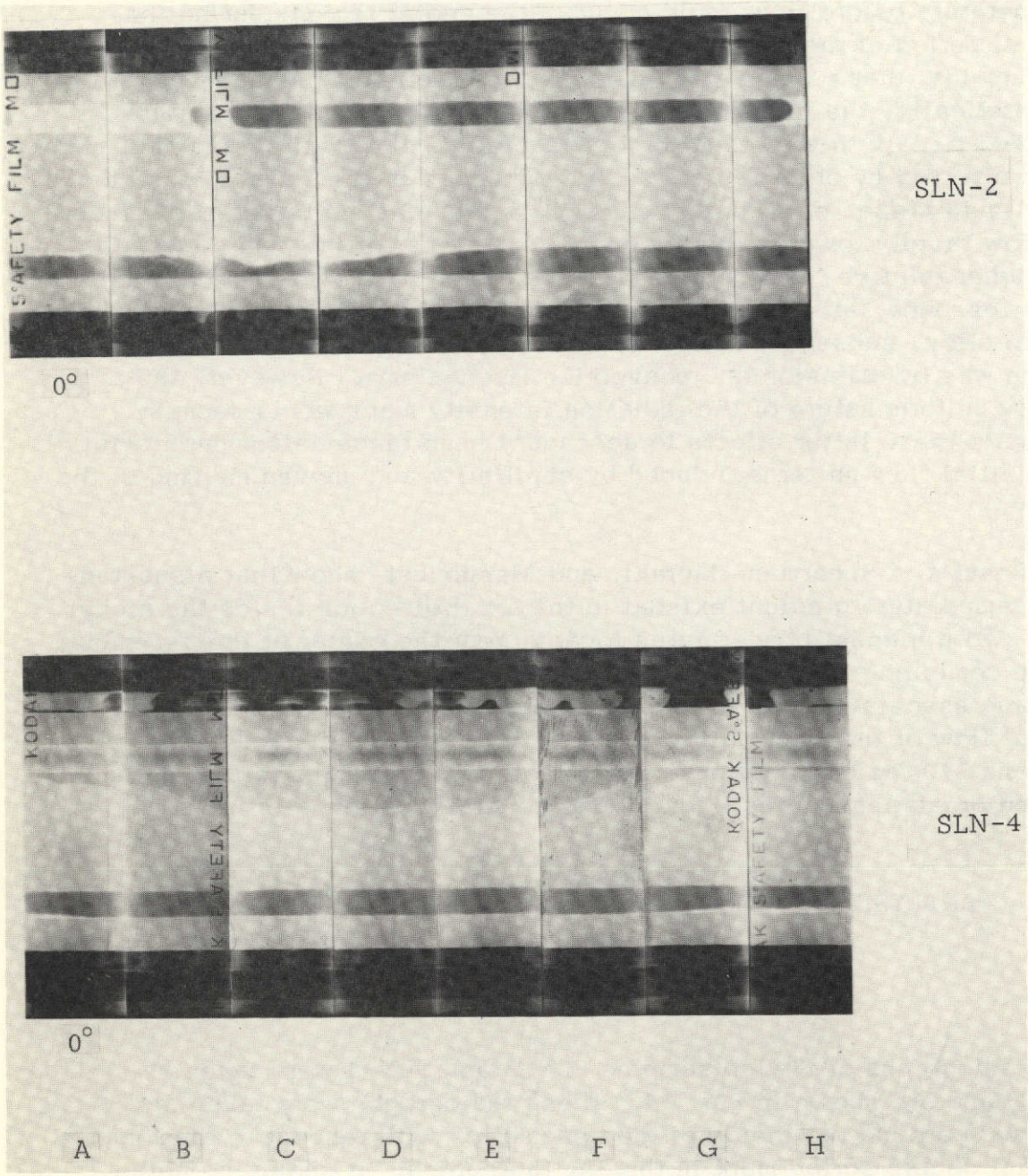

Figure 14. Radiographs of Skylab-II Assemblies SLN-2 and SLN-4

Upon brazing sample SLN-2 on Skylab, all but two small fillets of braze flowed out of the upper and lower ring grooves. A rather large void area was observed outside the ring groove containing the isotope tracer pellet (see radiograph sections E, F, G, and H near the lettered end). The radiograph for sample SLN-4 shows that all but a small fillet of braze flowed from the lower ring groove. The upper ring groove appears to have some braze remaining. In both samples SLN-2 and SLN-4, braze flowed outside the sleeve between the nickel tube and the wedge rings; this observation was unique to samples brazed in a near-zero gravity environment, as will be shown later, and had an effect on the movement of the tracer material.

Autoradiographs

Autoradiographs were taken at MSFC on both samples SLN-2 and SLN-4 by wrapping Kodak type M film around the nickel ferrule for a total exposure time of 40 hours in a light-free environment. These autoradiographs were developed and then positive prints were made as shown in Fig. 15. In these autoradiographs the darker areas correspond to higher levels of radioactivity. The 360° azimuth represents the circumference of the nickel sleeve, and the original position of the tracer-containing pellet is marked on the print. The autoradiograph for sample SLN-2 shows that the tracer alloy flowed mainly in a circumferential direction to areas at an azimuth of about 180° from the original tracer pellet location (0°). Most of the radioactivity is located in proximity to the pellet ring groove. An area of low radioactivity content can be seen just inside the tracer pellet location near the "upper" braze ring groove. After brazing at zero gravity, the tracer alloy in sample SLN-4 appeared to be concentrated in two areas; one above and the other below the tracer pellet location.

Helium Leak Testing

ORNL was requested to determine the over-all integrity of the braze joints in Skylab samples SLN-2 and SLN-4 by helium leak detection techniques. This was accomplished by clamping an assembly inside a rubber tube, blanking off one end with a rubber stopper, and connecting the tube to the vacuum system of a Veeco MS-12 leak detector. The assembly was then checked to see whether helium would pass through the braze joint at any point. Both samples SLN-2 and SLN-4 demonstrated leak tight braze joints as no helium could be detected even on the most sensitive scale (10^{-10} atm cc/sec).

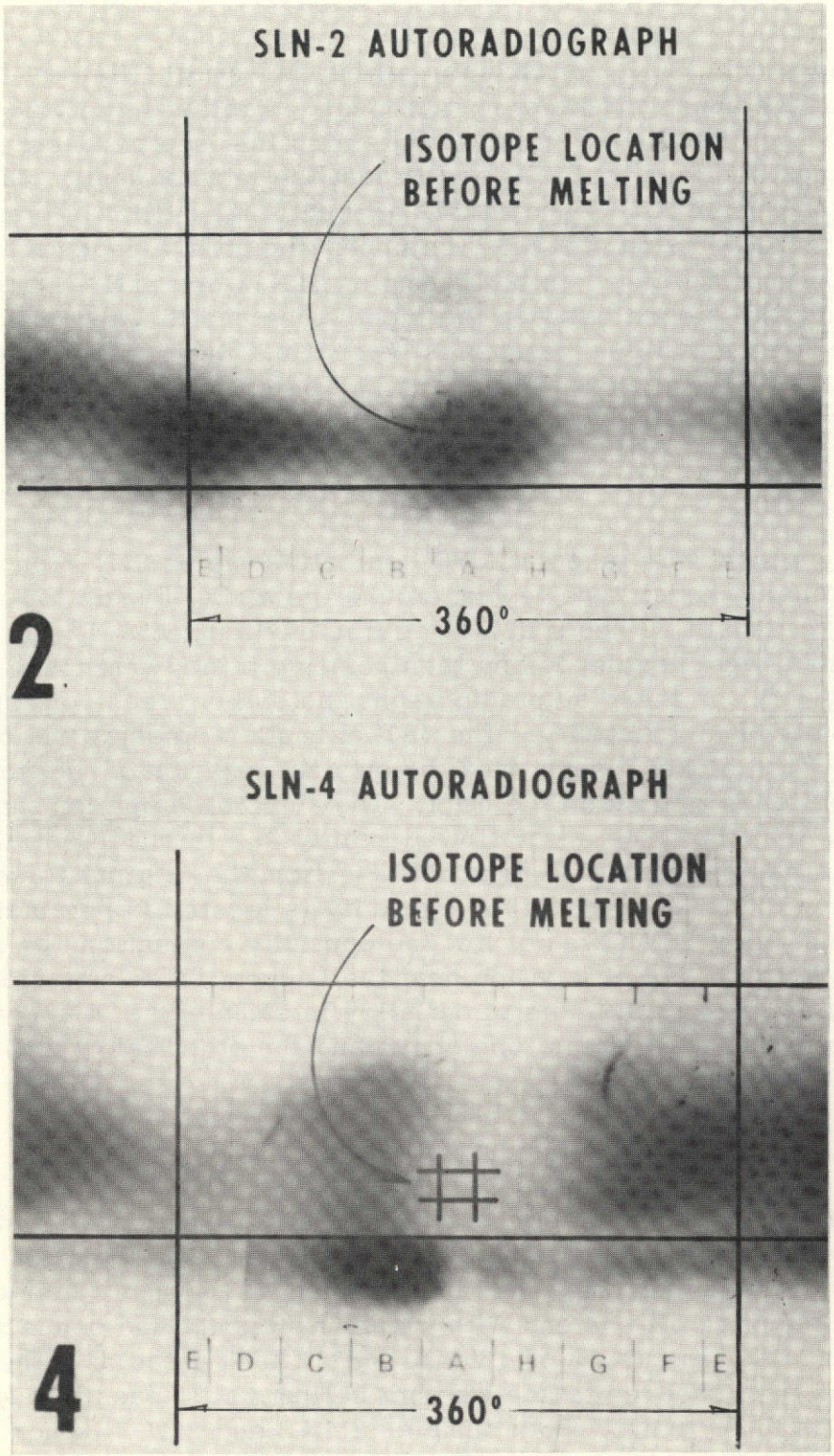

Figure 15. Autoradiographs of Skylab-II Assemblies SLN-2 and SLN-4

Sectioning

The SLN-2 and SLN-4 assemblies were sectioned into rings for radiation intensity mapping measurements by using electrical discharge machining (EDM). This technique was used in preference to sectioning on a lathe or with an abrasive cut-off wheel because better transverse sections with excellent parallel faces could be cut. EDM also had the advantage of producing an extremely shallow heat-affected or cold-worked surface. Figure 16 shows the two Skylab samples before sectioning; Figs. 17 and 18 give the sectioning plan for the two samples.

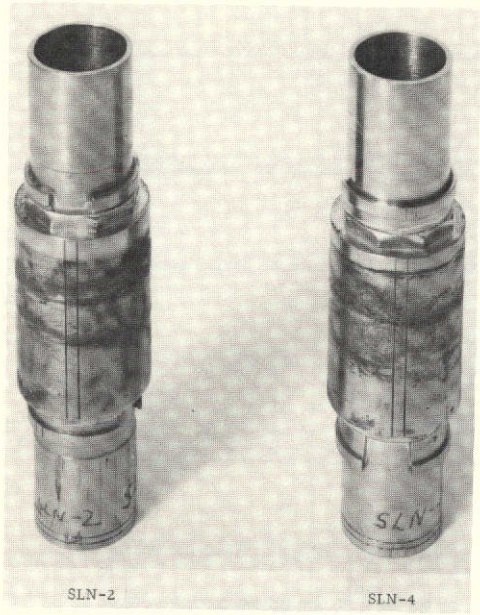

Figure 16. Photograph of Skylab-II Assemblies SLN-2 and SLN-4 Before Sectioning

Each section location is shown both in inches and millimeters as measured from the zero reference plane on the sleeve towards the scribed end. A kerf of ~0.025 in. (0.064 cm) is noted on the figures which was created by each cut using the 0.020-in. (0.051 cm) EDM electrode made of brass sheet. A "dot" code was used to label each ring so as to locate the specific section and its orientation. The dots were punched in the vicinity of the longitudinally scribed double lines. Multiple dots (two for sample SLN-2 and three for sample SLN-4) just outside the double scribe line lie closest to the cut surface that faced the scribed end (circumferential scribe marks) of the assembly. Therefore these dots provide the orientation of each ring section. The one, two, or

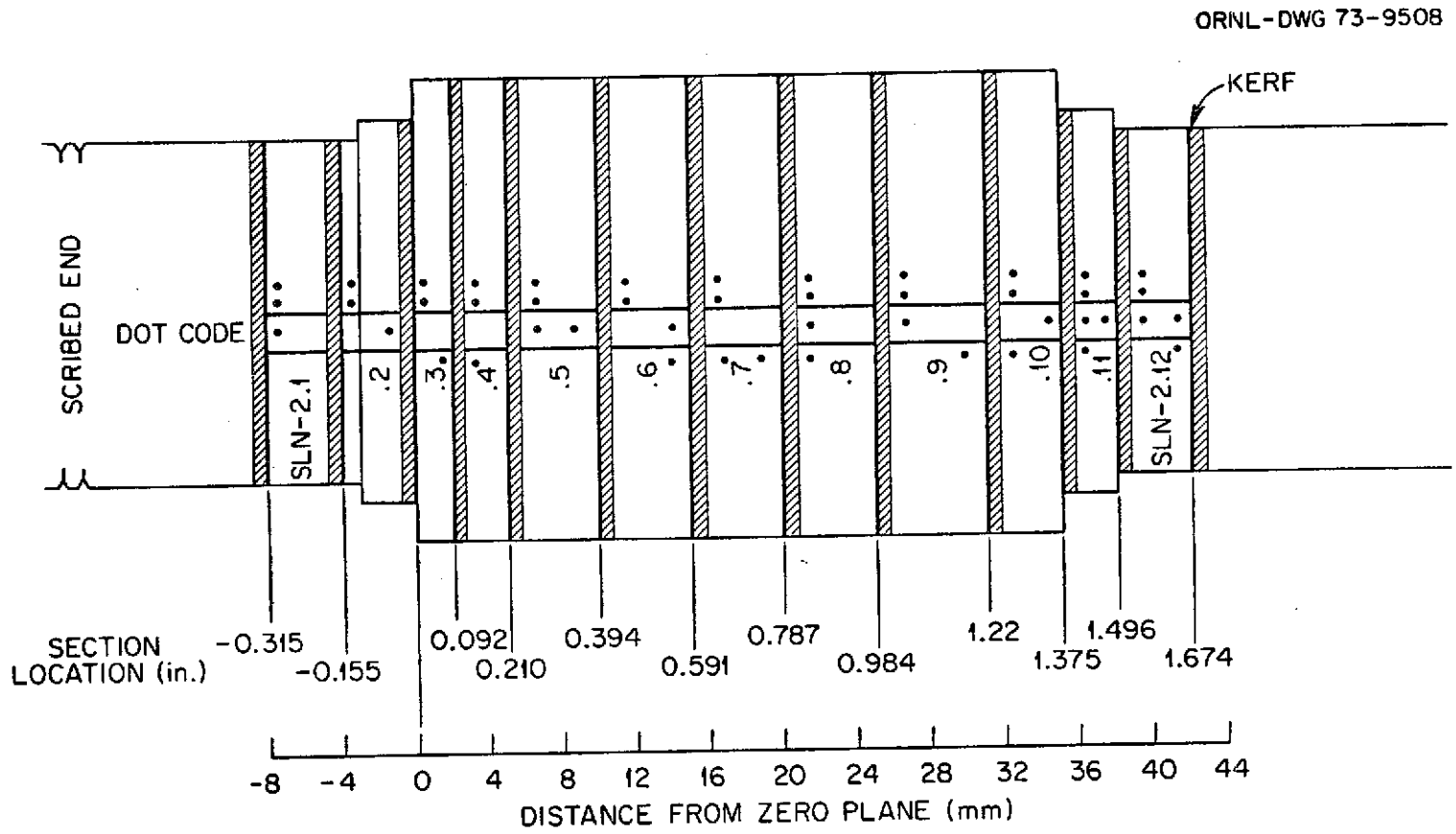

Figure 17. Sectioning Plan for SLN-2

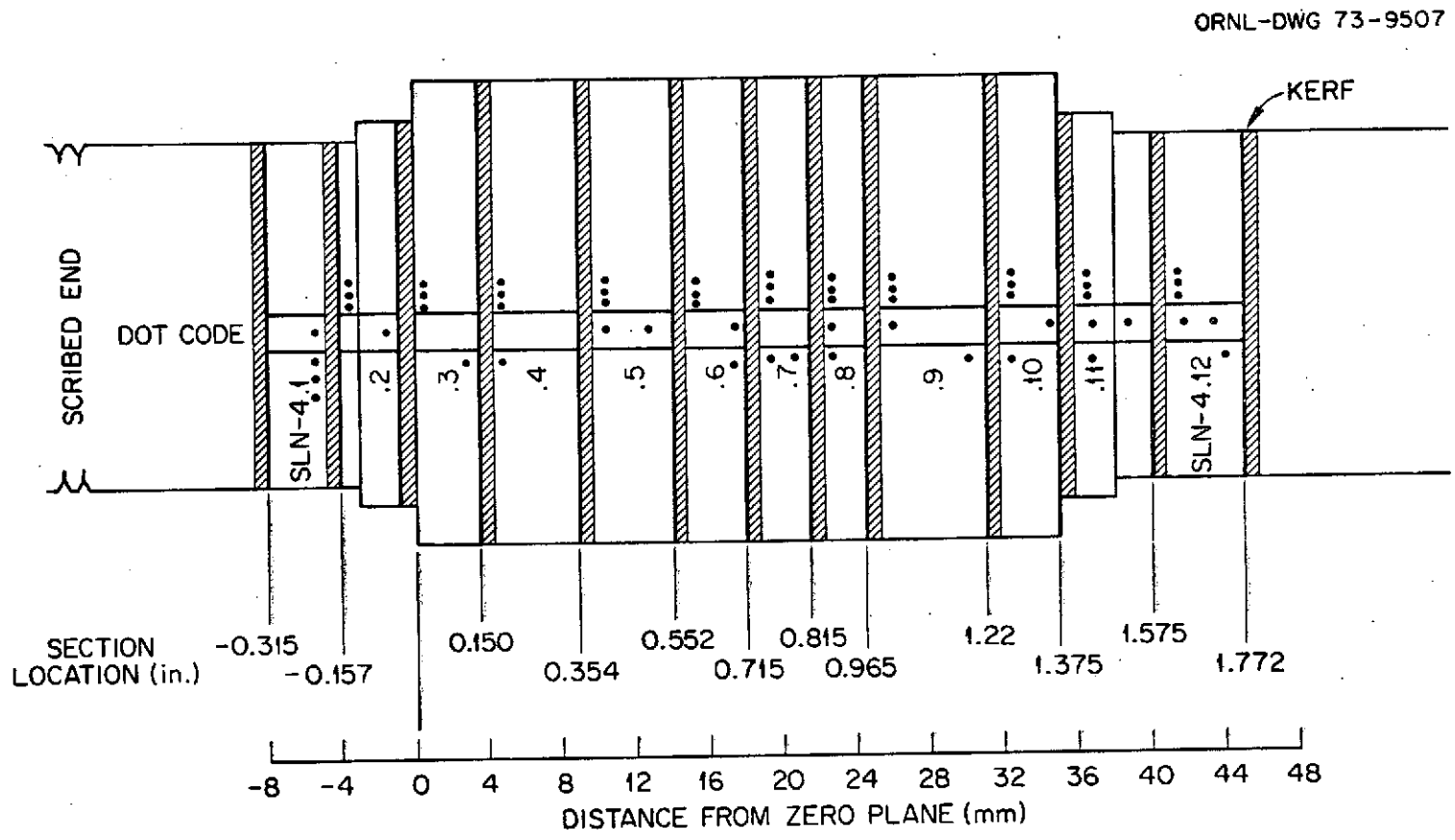

Figure 18. Sectioning Plan for SLN-4

three dot arrays located inside the longitudinal double scribed lines and on the side opposite the orientation dots give, by their arrangement, the location of each ring before cutting. One discrepancy should be noted for sample section SLN-4.1 in which the orientation dots were inadvertently punched on the wrong side. The true orientation of that section with relation to the dots and the assembly is shown in Fig. 18.

Radiation Intensity Maps

SLN-2. The radiation intensity map for sample SLN-2 is given in Fig. 19. This sample had a nominal annulus clearance of 0.010 in. (0.025 cm). As mentioned previously, some of the braze alloy flowed outside the nickel ferrule in the samples brazed in space (see Fig. 14). The effect of this extraneous flow is also shown by the movement of the tracer alloy which extended outside the zero reference plane to areas with negative distance values. However, most of the tracer alloy was concentrated on either side of the ring groove from an azimuth of approximately 40°, moving to the left, to 200°. An area of slight activity was found in the "upper" ring groove associated with a fillet of braze material. These results agree with those observed in the autoradiograph (see Fig. 15) for sample SLN-2 showing high radioisotope content along the "lower" ring groove.

SLN-4. The intensity map for sample SLN-4, having a 0.000-0.030 in. (0.000-0.076 cm) taper annulus, is given in Fig. 20. As before, the braze extended beyond the nickel ferrule, and moderate concentrations of the radioisotope were detected outside the ferrule edge at negative distance values. However, most of the ^{110}Ag tracer isotope was concentrated in areas above and below the tracer ring groove at an azimuth of approximately 280°. Since SLN-4 was a taper-gap sample, it must again be remembered that the lower concentration area inside the ring groove actually gave higher radiation intensity values than the high concentration area outside the groove, but these latter values were normalized by dividing by a smaller volume increment. With this normalization in mind, comparison of the tracer map in Fig. 20 to the autoradiograph in Fig. 15 can be made. Both the map and autoradiograph show the presence of two regions of intense radioactivity, and they agree with respect to their azimuthal location. One of the main differences between the braze flow in the tapered annulus sample brazed in space and a similar sample brazed on earth was the lack of the "water leveling" effect in the near-zero gravity experiments. Large islands of braze alloy were observed in the 0.030 in. (0.076 cm) gap end of

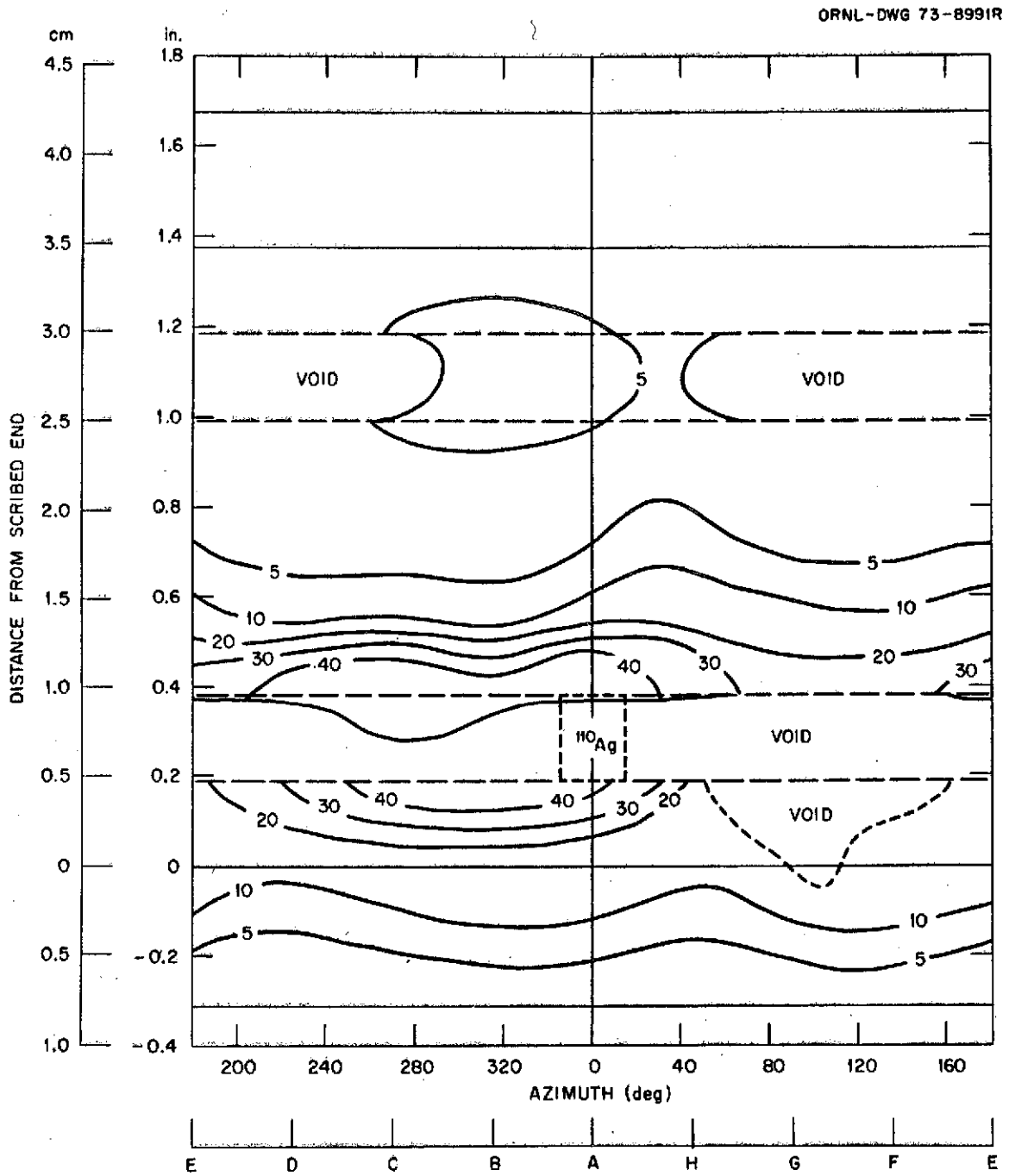

Figure 19. Radiation Intensity Map for SLN-2
Intensity units: (counts/sec · in.^{3}) x 10^{-4}

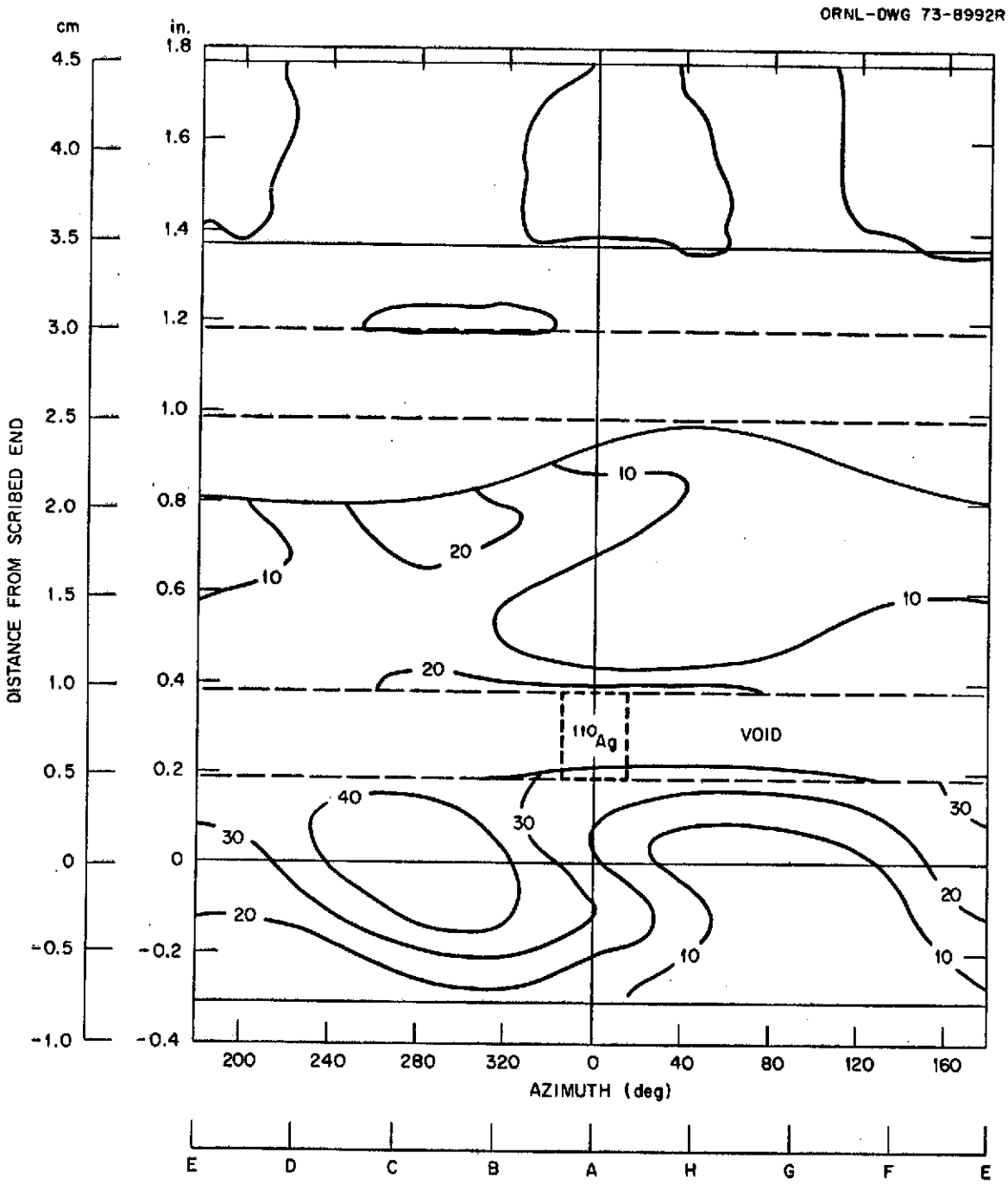

Figure 20. Radiation Intensity Map for SLN-4
Intensity units: (counts/sec · in.^{3}) x 10^{-4}

sample SLN-4; similar islands were entirely absent in samples IMN-2 and MCN-4 (Figs. 12 and 13, respectively). As with the ground-test samples, areas void of braze alloy did not show radiation intensity concentrations above the background level.

Discussion

Radioisotope tracer mapping of Skylab samples SLN-2 and SLN-4 showed very interesting differences and similarities when compared with similar maps of ground-test samples. One significant difference was the enhanced braze alloy flow (with subsequent increased movement of tracer alloy) observed in the samples brazed in space under near-zero gravity conditions. Radioactivity was observed for both samples SLN-2 and SLN-4 well outside of the ferrule region on the double-scribed or tracer pellet end. With gravitational forces absent, capillarity of surface forces were unopposed, resulting in rather dramatic increased flow of the braze alloy. Another difference due to the absence of gravity was manifested in sample SLN-4, a taper annulus sample, which demonstrated the absence of a braze "leveling" effect noted on ground-test samples; islands of braze alloy filled regions having very large gap widths. In some respects, the radiation intensity maps for the Skylab samples SLN-2 and SLN-4 were very similar to those obtained from earth samples. The tracer alloy moved initially towards the thermally hot regions near the igniters. In the Skylab flight package, the igniters were located near azimuth locations of 45° and 225° with respect to the tracer pellet location at 0° (see Fig. 3b). In both tracer maps (Figs. 19 and 20). virtually all of the radioisotope was found in regions between an azimuth of 225° and 45°. Braze fillets containing ^{110}Ag that remained in the braze ring grooves of sample SLN-4 (see Fig. 20) cannot be explained by gravitational effects, as in the ground samples, and must be a result of surface and thermal forces. The ^{110}Ag tracer maps for all of NASA M-552 braze assemblies suggest that such tracing can provide a picture of the thermal history for any particular assembly as well as accurate braze alloy flow information. Since no other analytical technique would provide this unique composite view of surface, gravitational, and thermal forces, radioisotope tracing proved useful in interpreting other metallurgical aspects of this experiment.

It is interesting to note that the areas void of solid braze alloy, yet wet by molten braze material, showed no residual tracer isotope activity. This observation would imply that the silver did not react nor adhere to the nickel surface.

CONCLUSIONS

1. The addition of a radioisotope tracer to the M-552 brazing experiment provided a unique picture of the thermal history of braze melting within the annulus as well as useful representation of the braze alloy flow pattern during the melting-solidification process.

2. Decreased resistance to flow of the Lithobraze BT (71.8% Ag, 28% Cu, 0.2% Li) was achieved in space. Alloy flow patterns, observed in samples brazed in a near-zero gravity field, extended beyond the ferrule annular region, while patterns observed in samples brazed in a unit gravity field were totally contained within the annulus.

3. Movement of the tracer alloy, induced by gravity, towards the bottom of the ring groove, originally containing the tracer, was absent in samples brazed in space.

4. Tracer alloy moved initially towards the regions near the thermite igniters where higher ferrule temperatures would be expected. Therefore, the initial flow pattern of braze alloy was the result of thermal effects.

5. Annular regions that contained braze material which subsequently flowed elsewhere, exhibited no residual radioactivity, thus indicating no silver surface deposits.

APPENDIX A

Sectioning Data for IMN-1

*Distance from sleeve edge at scribed end.
Detector diameter = 0.13 in. (0.33 cm).

Section No.	*Section Location in. (cm)	Azimuth Location deg.	Section Thickness in. (cm)	Gap Width in. (cm)	Volume Correction Factor	Volume x 10^{-4} in.^{3} (x 10^{-3} cm^3)
1	0.07 (0.18)	0-360	0.070 (0.178)	0.010 (0.025)	1	0.91 (1.49)
2	0.17 (0.43)	0-360	0.064 (0.163)	0.010 (0.025)	1	0.83 (1.36)
3	0.30 (0.76)	0-360	0.020 (0.051)	0.062	0	0 (0)
4	0.40 (1.02)	0-360	0.050 (0.127)	0.010 (0.025)	0.5	0.33 (0.54)
5	0.48 (1.22)	0-360	0.050 (0.127)	0.010 (0.025)	1	0.65 (1.07)
6	0.57 (1.45)	0-360	0.050 (0.127)	0.010 (0.025)	1	0.65 (1.07)
7	0.68 (1.73)	0-360	0.050 (0.127)	0.010 (0.025)	1	0.65 (1.07)
8	0.81 (2.06)	0-360	0.074 (0.188)	0.010 (0.025)	1	0.96 (1.57)
9	0.88 (2.24)	0-360	0.040 (0.102)	0.010 (0.025)	1	0.52 (0.85)
10	0.96 (2.44)	0-360	0.060 (0.152)	0.062 (0.157)	0.6	2.90 (4.75)
11	1.13 (2.87)	0-360	0.115 (0.292)	0.010 (0.025)	0.5	0.75 (1.23)
12	1.24 (3.15)	0-360	0.120 (0.305)	0.010 (0.025)	0.5	0.78 (1.28)

APPENDIX B

Sectioning Data for IMN-2

*Distance from sleeve edge at scribed end.
Detector diameter = 0.13 in. (0.33 cm).

Section No.	*Section Location in. (cm)	Azimuth Location deg.	Section Thickness in. (cm)	Gap Width in. (cm)	Volume Correction Factor	Volume $\times 10^{-4}$ in.^{3} ($\times 10^{-3}$ cm^3)
1	0.85 (2.16)	0-360	0.080 (0.203)	0.016 (0.041)	1	1.66 (2.72)
2	0.75 (1.91)	0-360	0.080 (0.203)	0.014 (0.036)	1	1.46 (2.39)
3	0.65 (1.65)	0-360	0.075 (0.191)	0.012 (0.030)	1	1.17 (1.92)
4	0.55 (1.40)	0-360	0.072 (0.183)	0.010 (0.025)	1	0.94 (1.54)
5	0.45 (1.14)	0-360	0.068 (0.173)	0.008 (0.020)	1	0.71 (1.16)
6	0.35 (0.89)	0-360	0.070 (0.178)	0.006 (0.015)	1	0.55 (0.90)

APPENDIX C

Sectioning Data for MCN-1

*Distance from sleeve edge at scribed end.
Detector diameter = 0.13 in. (0.33 cm).

Section No.	*Section Location in. (cm)	Azimuth Location deg.	Section Thickness in. (cm)	Gap Width in. (cm)	Volume Correction Factor	Volume x 10^{-4} in.^{3} (x 10^{-3} cm^3)
F	0.11 (0.28)	0-360	0.105 (0.267)	0.010 (0.025)	1	1.37 (2.25)
E4	0.20 (0.51)	0-360	0.050 (0.127)	0.010 (0.025)	1	0.65 (1.07)
E3	0.31 (0.79)	0-360	-	-	0	0 (0)
E2	0.41 (1.04)	200-160	0.065 (0.165)	0.010 (0.025)	0.5	0.42 (0.69)
		160-200	0.065 (0.165)	0.010 (0.025)	1	0.85 (1.39)
E1	0.52 (1.32)	0-360	0.080 (0.203)	0.010 (0.025)	1	1.04 (1.70)
D	0.62 (1.57)	0-360	0.072 (0.183)	0.010 (0.025)	1	0.94 (1.54)
C2	0.67 (1.70)	0-360	0.030 (0.076)	0.010 (0.025)	1	0.39 (0.64)
C1	0.80 (2.03)	0-360	0.100 (0.254)	0.010 (0.025)	1	1.30 (2.13)
B	0.90 (2.29)	0-360	0.072 (0.183)	0.010 (0.025)	1	0.94 (1.54)

APPENDIX D

Sectioning Data for MCN-3

*Distance from sleeve edge at scribed end.
Detector diameter = 0.13 in. (0.33 cm).

Section No.	*Section Location in. (cm)	Azimuth Location deg.	Section Thickness in. (cm)	Gap Width in. (cm)	Volume Correction Factor	Volume x 10^{-4} in.^{3} (x 10^{-3} cm^3)
1	0.10 (0.25)	0-360	0.110 (0.279)	0.010 (0.025)	1	1.43 (2.34)
2	0.25 (0.64)	40-320	0.118 (0.300)	0.010 (0.025)	0.5	1.53 (2.51)
		320-40	0.118 (0.300)	0.065 (0.165)	0.13	9.97 (16.33)
3	0.40 (1.02)	40-320	0.119 (0.302)	0.010 (0.025)	0.5	1.55 (2.54)
		320-40	0.119 (0.302)	0.065 (0.165)	0.13	10.06 (16.49)
4	0.50 (1.27)	0-360	0.078 (0.198)	0.010 (0.025)	1	1.01 (1.66)
5	0.64 (1.63)	0-360	0.110 (0.279)	0.010 (0.025)	1	1.43 (2.34)
6	0.78 (1.98)	0-360	0.100 (0.254)	0.010 (0.025)	1	1.30 (2.13)
7	0.92 (2.34)	0-360	0.094 (0.239)	0.010 (0.025)	1	1.22 (2.00)

APPENDIX E

Sectioning Data for MCN-4

*Distance from sleeve edge at scribed end.
Detector diameter = 0.13 in. (0.33 cm).

Section No.	*Section Location in. (cm)	Azimuth Location deg.	Section Thickness in. (cm)	Gap Width in. (cm)	Volume Correction Factor	Volume x 10^{-4} in.^{3} (x 10^{-3} cm^3)
L	0.12 (0.30)	0-360	0.118 (0.300)	0.002 (0.005)	1	0.31 (0.51)
K2	0.41 (1.04)	0-360	0.070 (0.178)	0.007 (0.018)	1	0.64 (1.05)
K1	0.51 (1.30)	0-360	0.060 (0.152)	0.009 (0.023)	1	0.70 (1.15)
J	0.62 (1.57)	0-360	0.080 (0.203)	0.011 (0.028)	1	1.14 (1.87)
I2	0.70 (1.78)	0-360	0.055 (0.140)	0.013 (0.033)	1	0.93 (1.52)
I1	0.79 (2.01)	0-360	0.060 (0.152)	0.015 (0.038)	1	1.17 (1.92)
H	0.90 (2.29)	0-360	0.080 (0.203)	0.017 (0.043)	1	1.77 (2.90)

APPENDIX F

Sectioning Data for SLN-2

*Distance from sleeve edge at scribed end.
Detector diameter = 0.13 in. (0.33 cm)

Section No.	*Section Location in. (cm)	Azimuth Location deg.	Section Thickness in. (cm)	Gap Width in. (cm)	Volume Correction Factor	Volume x 10^{-4} in.^{3} (x 10^{-3} cm^3)
1	-0.315 (-0.800)	0-360	0.147 (0.373)	0.002 (0.005)	1	0.38 (0.62)
2	-0.155 (-0.394)	0-360	0.134 (0.340)	0.002 (0.005)	1	0.35 (0.57)
3	0.092 (0.234)	120-60	0.092 (0.234)	0.010 (0.025)	1	1.20 (1.97)
		60-120	0.092 (0.234)	0.010 (0.025)	0	0 (0)
4	0.210 (0.533)	160-50	0.098 (0.249)	0.010 (0.025)	1	1.27 (2.08)
		50-160	0.098 (0.249)	0.010 (0.025)	0	0 (0)
5	0.394 (1.001)	0-360	0.168 (0.427)	0.010 (0.025)	0.6	2.18 (3.57)
6	0.591 (1.501)	0-360	0.185 (0.470)	0.010 (0.025)	1	2.41 (3.95)
7	0.787 (1.999)	0-360	0.177 (0.450)	0.010 (0.025)	1	2.30 (3.77)
8	0.984 (2.499)	0-360	0.186 (0.472)	0.010 (0.025)	1	2.42 (3.97)
9	1.220 (3.099)	0-360	0.213 (0.541)	0.010 (0.025)	1	2.77 (4.54)
10	1.375 (3.493)	0-360	0.125 (0.318)	0.010 (0.025)	1	1.63 (2.67)
11	1.496 (3.780)	0-360	0.087 (0.221)	0.002 (0.005)	1	0.23 (0.38)
12	1.674 (4.252)	0-360	0.138 (0.351)	0.002 (0.005)	1	0.36 (0.59)

APPENDIX G

Sectioning Data for SLN-4

*Distance from sleeve edge at scribed end.
Detector diameter = 0.13 in. (0.33 cm)

Section No.	*Section Location in. (cm)	Azimuth Location deg.	Section Thickness in. (cm)	Gap Width in. (cm)	Volume Correction Factor	Volume $\times 10^{-4}$ in.^{3} ($\times 10^{-3}$ cm^3)
1	-0.315 (-0.800)	0-360	0.140 (0.356)	0.002 (0.005)	1	0.36 (0.59)
2	-0.157 (-0.399)	0-360	0.140 (0.356)	0.002 (0.005)	1	0.36 (0.59)
3	0.150 (0.381)	0-360	0.150 (0.381)	0.002 (0.005)	1	0.39 (0.64)
4	0.354 (0.899)	0-360	0.186 (0.472)	0.005 (0.013)	1	1.21 (1.98)
5	0.552 (1.402)	0-360	0.170 (0.432)	0.009 (0.022)	1	1.99 (3.26)
6	0.715 (1.816)	0-360	0.130 (0.330)	0.012 (0.030)	1	2.03 (3.33)
7	0.850 (2.159)	0-360	0.106 (0.269)	0.015 (0.038)	1	2.07 (3.39)
8	0.965 (2.451)	320-140	0.088 (0.224)	0.017 (0.043)	1	1.95 (3.20)
		140-320	0.088 (0.224)	0.017 (0.043)	0	0 (0)
9	1.220 (3.099)	260-320	0.245 (0.622)	0.021 (0.053)	1	6.69 (10.96)
		320-260	0.245 (0.622)	0.021 (0.053)	0	0 (0)
10	1.375 (3.493)	260-340	0.125 (0.318)	0.025 (0.064)	1	4.06 (6.65)
		340-260	0.125 (0.318)	0.025 (0.064)	0	0 (0)
11	1.575 (4.001)	340-60 120-220	0.165 (0.419)	0.002 (0.005)	1	0.43 (0.70)
		220-340 60-120	0.165 (0.419)	0.002 (0.005)	0	0 (0)
12	1.772 (4.501)	0-360	0.175 (0.445)	0.002 (0.005)	1	0.46 (0.75)

REFERENCES

1. Radiological Health Handbook, U. S. Department of Health, Education and Welfare, No. PB 121784R, Sept. 1960, p. 301.

2. Nuclear Data Sheets, Vol. 5, No. 5, May 1971.

3. J. W. Spearman, T. Muraki, and K. Masubuchi, First Interim Report on Phase B of Thermal Analysis of M-552 Experiment for Materials Processing in Space, Dept. Ocean Engineering, MIT, Jan. 15, 1973.

☆U.S. GOVERNMENT PRINTING OFFICE 1974 — 640-448 / 155 REGION NO. 4